

Comparative Study of Notched Circular Slotted and Rectangular Slotted Microstrip patch antennas (MPA) for wideband applications

Parul Bansal*, Ekambir Sidhu**, Sonia Goyal***

*(Department of Electronics and Communication, Punjabi University, Patiala
Email: parul.bansal4900@gmail.com)

** (Department of Electronics and Communication, Punjabi University, Patiala
Email: ekambirsidhu1988@gmail.com)

*** (Department of Electronics and Communication, Punjabi University, Patiala
Email: goyalsonia_82@yahoo.co.in)

ABSTRACT

In this paper, two equivalent Microstrip patch antenna designs for wideband applications have been proposed. The antennas are designed using radiating patch on one side of the dielectric substrate (FR4) and a reduced ground plane on the other side of substrate. Among two antennas, one antenna has a notched circular slot on the patch and other has a rectangular slotted patch. A comparative analysis of both antennas has been carried out in terms of various antenna parameters such as return loss (dB), bandwidth, gain and VSWR. The antennas are designed and simulated using CST Microwave Studio 2010. Both antennas cover frequency bands corresponding to IMT, WLAN and Wi-MAX applications. MPA with notched circular slot provides good return loss of -41.57dB at 4.5GHz and -46.78dB at 6.2GHz in comparison to rectangular slot MPA which provides a return loss of -26.45dB at 4.7GHz and -24.36 dB at 6.2 GHz. The antennas are approximately equivalent in terms of bandwidth (2.7GHz). The gain is sufficiently large at high resonant frequencies and VSWR is less than two for both the antenna designs.

Keywords - Microstrip patch antenna, Notched circular slot, Rectangular slot, Reduced ground plane, Return loss, VSWR

I. INTRODUCTION

Microstrip antenna, also acknowledged as patch antenna is usually fabricated on a dielectric substrate which acts as an intermediate between a ground plane at the bottom side of substrate and a radiating patch on the top of substrate [1]. The patch is primarily made of perfect electric conductor (PEC) material like copper. The patch can be of several shapes like rectangular, circular, triangular, elliptical, ring, Square and many more but commonly, rectangular shape is widely used [1]. While designing an antenna, the most important parameter is to select a substrate. The substrate consists of a dielectric material which perturbs the transmission line and electrical performance of antenna. The size of an antenna depends on the dielectric constant of substrate. Higher the dielectric constant, lower is the size of antenna [2]. Varieties of substrates with different dielectric constants are available but fire resistance 4 (FR4) material with dielectric constant of 4.4 has been used in these antenna designs. The antenna can be fed by various methods like coaxial feed, proximity coupled microstrip feed and aperture

coupled microstrip feed [3]. Feeding is a mean to transfer the power from the feedline to the patch which itself acts as radiator. Microstrip line feed has been used in MPA designs because it is relatively simple to fabricate [3].

Microstrip antenna have been commonly used for wireless applications because of its miniaturization, low cost, light weight, better efficiency, ease of installation, ease of mobility, and is relatively inexpensive to manufacture from printed circuit board (PCB) of specific characteristics and dimensions. However, the MPA suffers from a drawback that it handles less power and has limited bandwidth [4].

The bandwidth of MPA can be improved by either using a slotted patch [5] [6] or a reduced ground plane [7] [8]. The slot on the patch can be of any shape like H-slot [9], E-slot [10], circle, rectangle etc. These techniques can also be used to improve the return loss along with bandwidth enhancement.

In this paper, it has been analyzed that by using circular slotted MPA and rectangular slotted MPA with reduced ground plane, the bandwidth gets

doubled in comparison to a simple MPA without slotting and with full ground plane. Different shapes of slots have different impact on antenna parameters. MPA with circular slot provides better return loss than MPA with rectangular slot.

II. ANTENNA GEOMETRY

Fig 1 represents the geometry of a notched circular slotted MPA. As shown in the Fig 1, the shape of patch is rectangular with a circular and rectangular slot simultaneously cut on it. The patch is fed by a Microstrip feed line of certain specified width.

Fig 2 depicts the configuration of rectangular slotted MPA having a rectangular slot cut on the radiating rectangular patch. The antennas are fabricated on FR4 substrate having relative permittivity of 4.4 and thickness of 1.6mm. The width of the feed line is adjusted to make sure that the impedance of antenna is 50 ohms. The bottom of the substrate consists of ground plane which is partially reduced to improve antenna bandwidth. The various dimensions of both antennas are listed in Table 1 and Table 2 respectively.

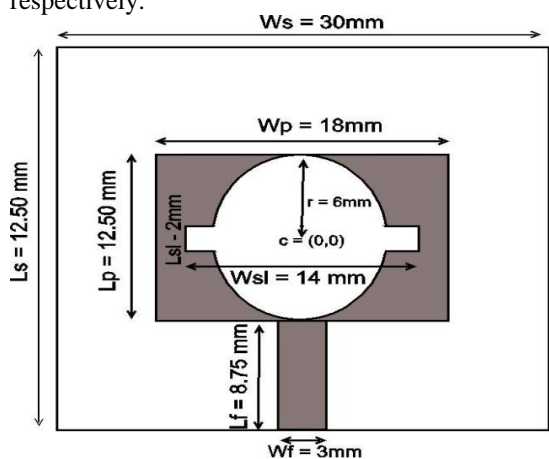


Fig 1(a): Top View of Notched Circular Slotted MPA

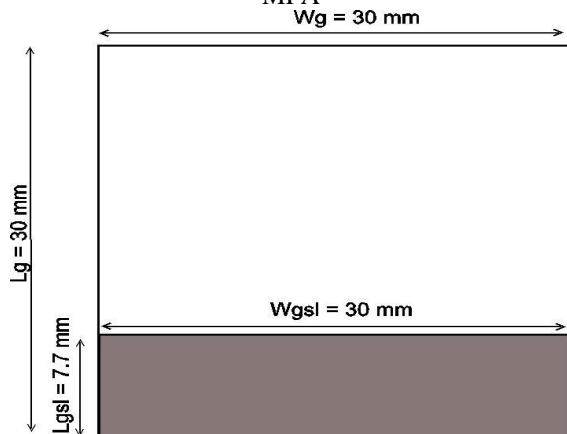


Fig 1(b): Bottom View of Notched Circular Slotted MPA

Table 1 Dimensions of notched circular slotted MPA

Antenna Parameter	Specification
Length of substrate (L_s)	30mm
Width of substrate (W_s)	30mm
Length of Patch (L_p)	12.50mm
Width of Patch (W_p)	18mm
Length of feed (L_f)	8.75mm
Width of feed (W_f)	3mm
Radius of circular slot (r)	6mm
Coordinates of Centre of circle (c)	(0,0)
Length of rectangular notch in circle (L_{sl})	2 mm
Width of rectangular notch in circle (W_{sl})	14mm

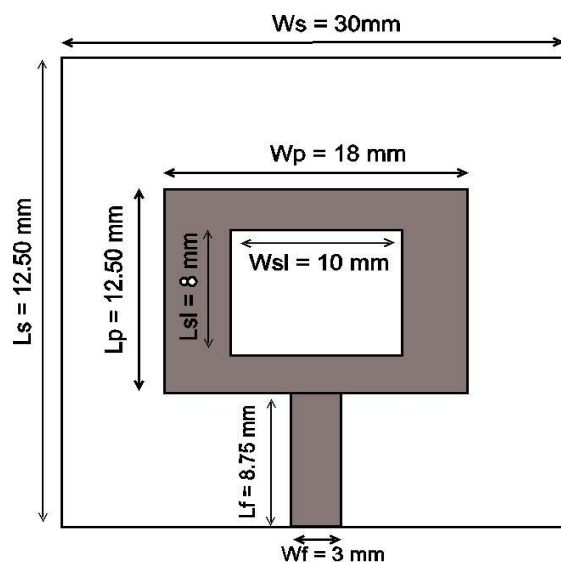


Fig 2(a): Top View of Rectangular Slotted MPA

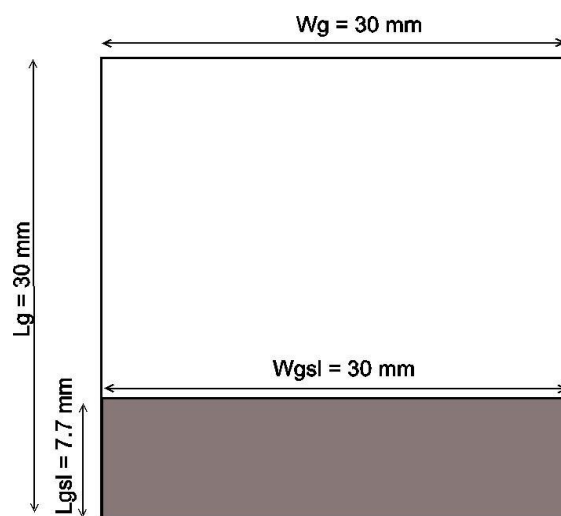


Fig 2(b): Bottom View of Rectangular Slotted MPA

Table 2: Dimensions of Rectangular Slotted MPA

Antenna Parameter	Specification
Length of substrate (L_s)	30mm
Width of substrate (W_s)	30mm
Length of Patch (L_p)	12.50mm
Width of Patch (W_p)	18mm
Length of feed (L_f)	8.75mm
Width of feed (W_f)	3mm
Length of slot (L_{sl})	8mm
Width of slot (W_{sl})	10mm

III. RESULTS AND DISCUSSIONS

The designed antennas have been simulated using CST Microwave Studio 2010 and the performance of the antenna has been analyzed in terms of return loss, VSWR, radiation pattern and gain. Meanwhile, the experimental results have been also obtained using E5071C ENA series network analyzer and concluded that the practical results approximately matches with the simulated theoretical results.

Fig 3 represents the simulated results of return loss for both antenna designs. It has been observed that the return loss for notched circular slot MPA is -41.57dB at 4.5GHz and -46.78dB at 6.2GHz and for rectangular slot MPA, return loss is -26.45dB at 4.7GHz and -24.36 dB at 6.2 GHz. Therefore, notched circular slot MPA provides better return loss i.e. amount of reflected power is less. The simulated bandwidth of the proposed antennas is same i.e. 2.7GHz

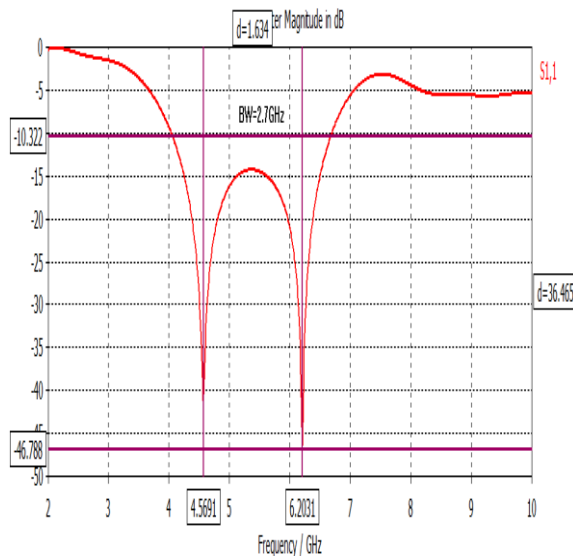


Fig 3(a): Return Loss Plot of Notched Circular Slot MPA

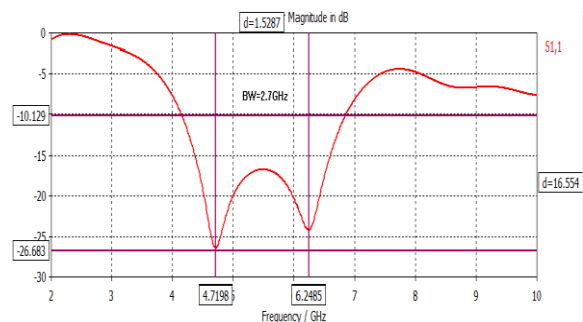


Fig 3(b): Return Loss Plot of Rectangular Slot MPA

Fig 4 shows the 3D radiation pattern for directivity of notched circular slotted MPA. The directivity at resonant frequencies has been obtained and analyzed. The directivity is 2.997dBi at 4.5GHz and 4.108 dBi at 6.2 GHz. It has been observed that directivity is better for higher resonant frequencies than lower frequencies.

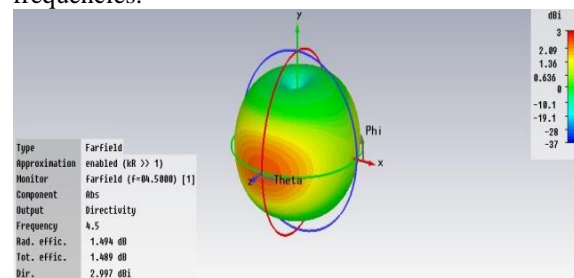


Fig 4(a): Directivity of Notched Circular Slot MPA at 4.5ghz

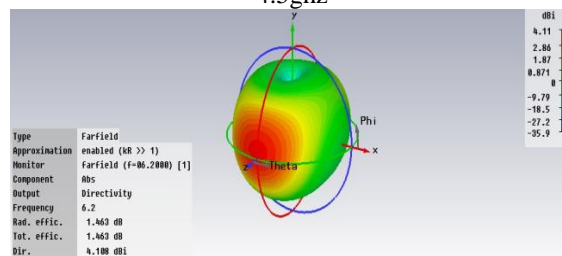


Fig 4(b): Directivity of Notched Circular Slot MPA at 6.2 GHz

Fig 5 depicts the 3D radiation pattern for directivity of rectangular slotted MPA. The directivity is 3.008 dBi at 4.7 GHz and 3.813 dBi at 6.2 GHz. The directivity is higher at high resonant frequency in comparison to lower frequencies.

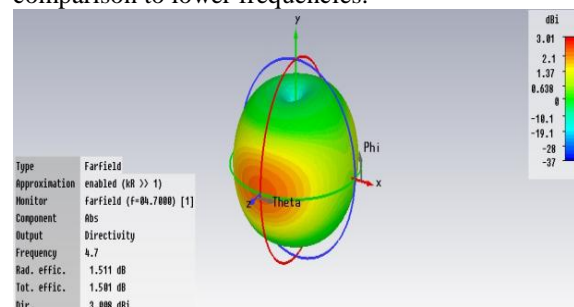


Fig 5(a): Directivity of Rectangular Slot MPA At 4.7 GHz

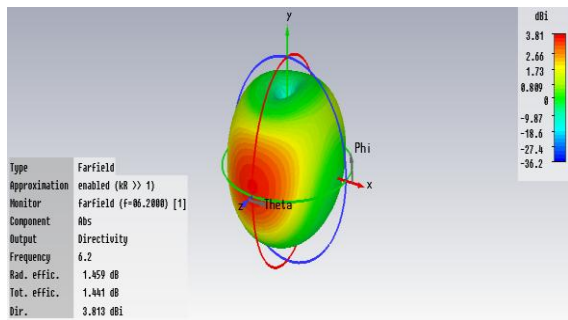


Fig 5(b): Directivity of Rectangular Slot MPA at 6.2 GHz

Fig 6 illustrates the simulated results of gain for notched circular slotted MPA. The 3D radiation pattern shows that the gain is 4.491 at 4.5 GHz and 5.57dBi at 6.2 GHz. It shows clearly that the value of gain is higher for high frequencies.

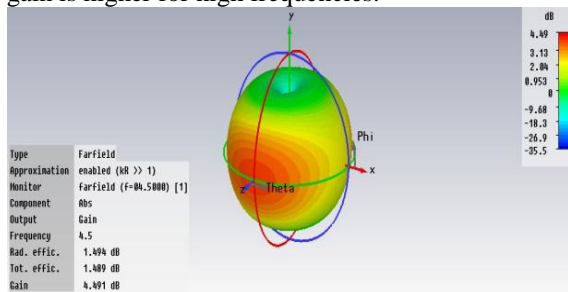


Fig 6(a): Gain of Notched Circular Slot MPA at 4.5 GHz

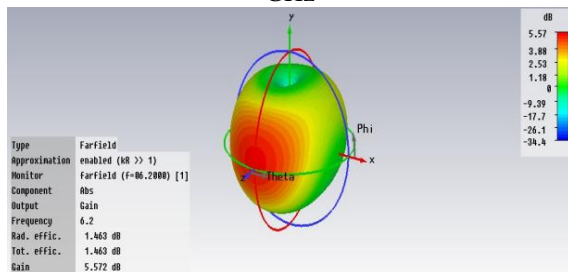


Fig 6(b): Gain of Notched Circular Slot MPA at 6.2 GHz

Fig 7 shows the 3D radiation pattern plot of gain for rectangular slotted MPA. The gain is 4.528 dB at 4.7 GHz and 5.271dB at 6.2 GHz. It can be concluded that the gain is better for higher frequencies as for circular slot MPA.

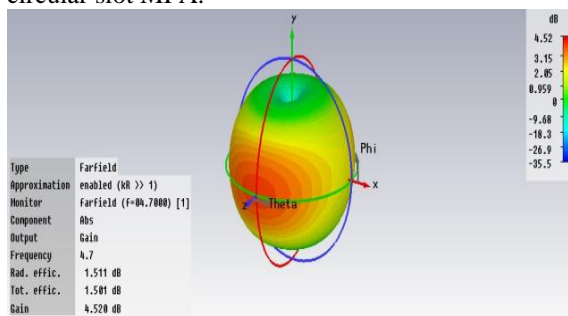


Fig 7(a) Gain Plot of Rectangular Slot MPA at 4.7 GHz

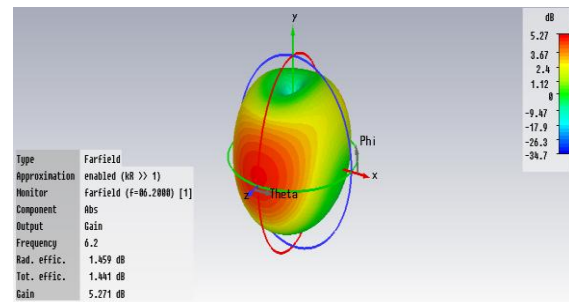


Fig 7(b): Gain Plot of Rectangular Slot MPA at 6.2 GHz

Fig 8 and Fig 9 depict the simulated VSWR plot for notched circular slotted MPA and rectangular slotted MPA respectively. Fig 8 shows that the VSWR at 4.5 GHz is 1.07 and 1.01 at 6.2 GHz and Fig.9 represents VSWR of 1.10 at 4.7 GHz and 1.13 at 6.2 GHz. The VSWR values corresponding to resonant frequencies is far below the satisfying criteria of VSWR (i.e. $VSWR < 2$).

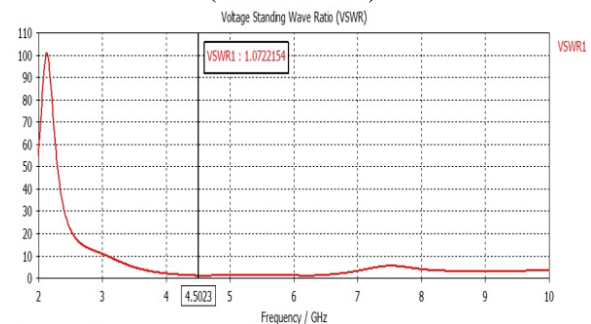


Fig 8(a): VSWR Plot of Notched Circular Slot MPA at 4.5 GHz

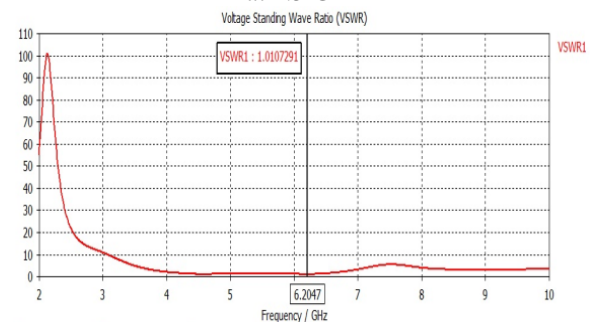


Fig 8(b): VSWR plot of Notched Circular Slot MPA at 6.2 GHz

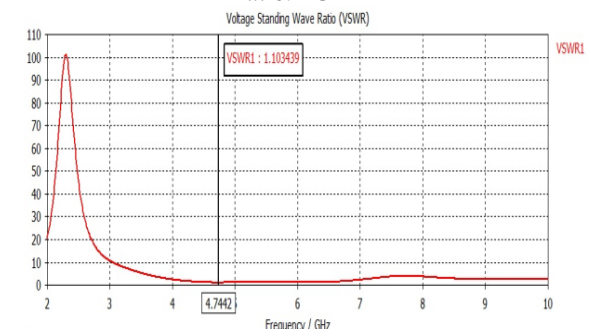


Fig 9(a): VSWR Plot of Rectangular Slot MPA at 4.7 GHz

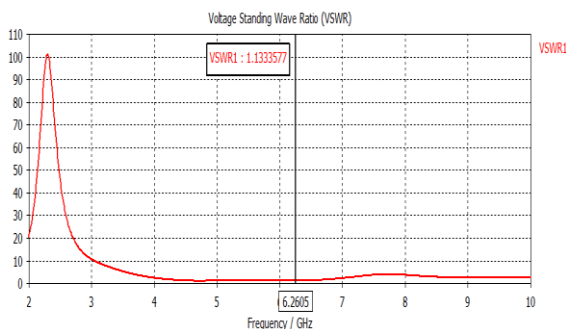


Fig 9(b): VSWR Plot of Rectangular Slot MPA at 6.2 GHz

IV. EXPERIMENTAL VERIFICATION

The proposed antennas has been physically designed as shown in Fig 10(a) and Fig 10(b) and tested using E5071C ENA series network analyzer. The experimental results of notched circular slotted MPA and rectangular slotted MPA is shown in Fig 11(a) and Fig 11(b) respectively.

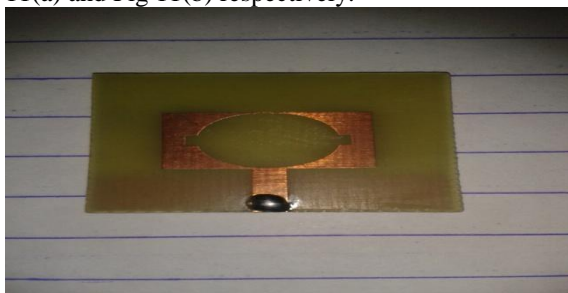


Fig 10(a): Notched Circular Slotted MPA

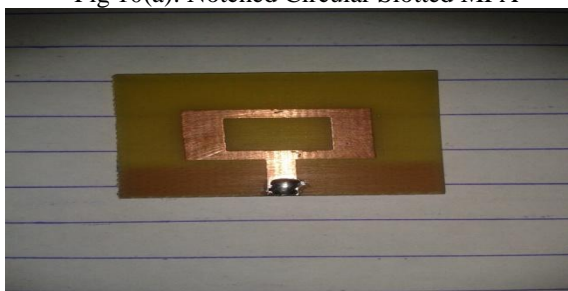


Fig 10(b): Rectangular Slotted MPA

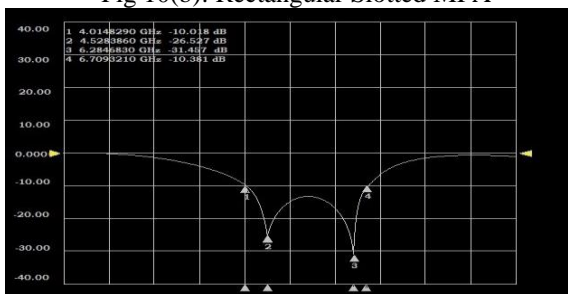


Fig 11(a): Experimental Results for Notched Circular Slotted MPA

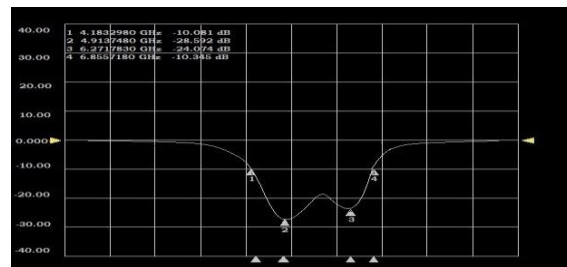


Fig 11(b): Experimental Results for Rectangular Slotted MPA

V. CONCLUSION

From the above discussion, it has been concluded that both the antennas (notched circular and rectangular slot MPA) have different impact on the antenna parameters. The antennas are equivalent in terms of the resonant frequencies and bandwidth. The selection of designed antenna for any application depends on the requirement. For example, rectangular slotted antenna is relatively simple to design whereas on the other side, if better return loss is required then circular slotted antenna can be designed. It can also be noticed that notched circular slotted MPA provides sharp well defined resonant frequencies in comparison to rectangular slotted MPA. The comparison of the proposed antennas in terms of various parameters has been shown in Table 3.

Table 3: Comparison of Simulated Antenna Designs

Antenna parameters	Notched Circular slotted MPA	Rectangular slotted MPA
Return loss	-41.57dB at 4.5GHz and -46.78dB at 6.2GHz	-26.45dB at 4.7GHz and -24.36 dB at 6.2 GHz
Bandwidth	2.701 GHz	2.720 GHz
Resonant frequencies	4.5 GHz , 6.2 GHz	4.7GHz,6.2 GHz
Sharpness of peaks	More sharp	Less sharp
Complexity in designing	More complex	Less complex

REFERENCES

- [1] Ritu Goyal, Y.K. Jain, "Compact Bow Shape Microstrip Patch Antenna with Different Substrates", *Proceedings of IEEE Conference on Information And Communication Technologies (ICT), 6505 (1), 2013, 1-9.*

- [2] C.A. Balanis, "Antenna Theory Analysis and Design", 2nd Edition, John Wiley & Sons, New York, 1996.
- [3] Neha Parmar, Manish Saxena, Krishnkant Nayak, "Review of Microstrip Patch Antenna for WLAN and WiMAX Application", *International Journal of Engineering Research And Applications*, 4 (1), January 2014, 168-171.
- [4] Sunil Kumar Rajgopal and Satish Kumar Sharma, "Investigations on Ultrawideband Pentagon Shape Microstrip Slot Antenna for Wireless Communications", *IEEE Transaction on Antennas and Propagation*, 57 (5), 2009, 1353-1359.
- [5] Govardhani Immadi, K. Swetha, M.Venkata Narayana, M.Sowmya, R.Ranjana, "Design of microstrip patch antenna for WLAN applications using Back to Back connection of Two E-Shapes", *International Journal of Engineering Research and Applications* , 2 (3), 2012,319-323.
- [6] Isha Puri, "Bandwidth and Gain increment of microstrip patch Antenna with Shifted elliptical Slot", *International Journal of Engineering Science and Technology (IJEST)*, 3(7), 2011, 5539-5545.
- [7] M. K. Mohamed Amin, M. T. Ali, S. Saripuden, A. A Ab Aziz, "Design of Dual Rectangular Ring Antenna with DGS Technique for Wireless Application", *IEEE Symposium on Wireless Technology and Applications (ISWTA)*, 2012.
- [8] Mohamed A. Hassanien and Ehab K .I. Hamad, "Compact Rectangular U-Shaped Slot Microstrip Patch Antenna For UWB Applications", *IEEE APS, Middle East Conference on Antennas and Propagation (MECAP), Cairo, Egypt, 20 (10), 2010.*
- [9] Sudhir Bhaskar & Sachin Kumar Gupta, "Bandwidth Improvement of Microstrip Patch Antenna Using H-Shaped Patch", *International Journal of Engineering Research and Applications*, 2 (1), 2012, 334-338.
- [10] B. Ramesh, V. Rajya Lakshmi, G. S. N. Raju, "Design of E-Shaped Triple Band Microstrip Patch Antenna", *International Journal of Engineering Research and Applications*, .3 (4), 2013, 1972-1974.

Laser Micromachining: Technology and Applications

Pradeep Kumar Agrawal

(Research Centre Imarat, DRDO, Vignyana Kancha, Hyderabad, India
Email: pradeep.kumar@rcilab.in)

ABSTRACT

Miniaturization is an important trend in many modern technologies. In view of this increasing trend toward miniaturization, micromachining becomes an important activity in the fabrication of microparts. Laser micromachining is controllable, highly accurate non contact machining and offers better flexibility in dimensional design of microproducts as it reduces deposition of recast layer and gives higher yield [1, 2]. Here, science behind the laser micromachining is explained and fabrication of optical vibration sensor with ultra short laser micromachining is also described.

Keywords: Laser micromachining, Laser ablation, Optical vibration sensor, ultra fast pulse laser

I. INTRODUCTION

Miniaturization is an important trend in many modern technologies. The requirement for material processing with micron or submicron resolution at high speed and low unit cost is an underpinning technology in nearly all industries manufacturing high-tech microproducts for biotechnological, microelectronics, telecommunication, MEMS, and medical applications. In view of this increasing trend toward miniaturization, micromachining becomes an important activity in the fabrication of microparts [1]. Various technologies such as mechanical micromachining (microdrilling and micromilling), focused ion beam micromachining, laser micromachining are being used in microfabrication. Ultra short pulses produce very high peak intensity ($> 10^{15}$ W/cm²) and deliver energy before thermal diffusion occurs, thus giving high efficiency and precision to the process without significant thermal degradation (melting, spatter, recrystallization, recasting of layer etc.) to the surrounding region. Ultra short laser can machine the transparent material like glass and can be used to fabricate a single mode waveguide in silicon.

II. LASER ABLATION

The ablation during laser processing refers to the material removal due to thermal and/or photochemical (nonthermal) interactions. In nonthermal ablation, the energy of the incident photon causes the direct bond breaking of the molecular chains in the organic materials resulting in material removal by molecular fragmentation without significant thermal damage. So the photon energy

must be greater than the bond energy. However, ablation also takes place when the photon energy is

less than the dissociation energy of the molecular bond as in the case of far ultraviolet radiation with longer wavelengths (correspondingly smaller photon energies), due to multiphoton absorption. In multiphoton mechanism, even though the energy associated with each photon is less than the dissociation energy of bond, the bond breaking is achieved by simultaneous absorption of two or more photons [1] [2].

During thermal ablation, the excitation energy is rapidly converted into heat, resulting in temperature rise. This temperature rise can cause the ablation of material by surface vaporization or spallation (due to thermal stresses). Thermal ablation mechanisms dominate the material removal during micromachining of metal and ceramics. One of the important considerations during the laser-material interaction during ablation is the thermal relaxation time (τ), which is related with the dissipation of heat during laser pulse irradiation and is expressed as [1]

$$\tau = d^2/4k \quad (1)$$

Where, d is absorption depth and k is thermal diffusivity. Thus, the two important parameters that determine the ease with which the ablation can be initiated are absorption coefficient (a) and thermal diffusivity (k). The large value of absorption coefficient and small value of thermal diffusivity generally provide the high ablation efficiency of a material. The ablation of material by confinement of laser energy in thin layer can also be facilitated by using short pulses (pulse time shorter than thermal

relaxation time). For longer pulses (pulse time longer than thermal relaxation time), the absorbed energy will be dissipated in the surrounding material by thermal processes. Thus, efficient ablation of the material during laser material interactions necessitates the lasers operating with short pulses. The ablation process is characterized by the ablation threshold, which corresponds to the laser fluence at which ablation starts. Different materials have different ablation thresholds primarily due to differences in the optical and thermal properties. The ablation rates during laser micromachining depend primarily on the laser parameters like wavelength, fluence, number of pulses and the materials properties.

III. LASER MICROMACHINING TECHNIQUES

The primary mechanisms of material removal during precision micromachining of materials are ablation and etching. The material removal by these mechanisms can be performed in various ways. The three important techniques of micromachining are described below:

a) Direct Writing Technique: The laser beam is focused on substrate surface. The micromachining of desired pattern is carried out either by translating the substrate with respect to the fixed laser beam or by scanning the laser beam. The important parameters during direct writing technique are size of the focus, the working distance, and the depth of focus. The minimum spot size is limited by the diffraction phenomenon.

b) Mask Projection Technique: A mask consisting of the shape of pattern to be produced on the substrate is illuminated with the laser light. The resolution of the features in the micromachined structures are determined by the mask and projection systems. Excimer lasers are extensively used for micromachining using the mask projection technique. In addition to the high resolution, better reproducibility and fine depth control are the main advantages of mask projection techniques. It allows the micromachining of large substrate areas.

c) Interference Technique: Laser interference technique involves splitting of a laser beam using a beam splitter followed by superposition of the beams to generate interference patterns. The interference pattern thus produced shows unique intensity variation which can be used for periodic micromachining of the substrates. The geometry of the interference patterns formed by the superposition of two or more coherent and linearly polarized beams depends on the wavelength and the angle between the beams. The intensity distribution resulting from the superposition of two linearly polarized beams with

their [1] E vectors in the x-direction can be expressed as:

$$I(x) = 2 I_0 [\cos(2\pi x/l) + 1] \quad (2)$$

$$l = \lambda/2\sin(\Theta/2) \quad (3)$$

Where, I_0 is intensity of a laser beam, λ is wavelength, Θ is angle between the beams, and l is periodicity of the two beam interference pattern.

IV. MACHINING WITH LONG PULSE LASERS

Heat deposited by the laser in the material, diffuses away during the pulse duration as laser pulse duration is greater than the diffusion time. This is desirable in laser welding but for micromachining heat diffusion into surrounding region is undesirable. The following are effects of heat diffusion:

- Heat diffusion decreases the efficiency of micromachining process as it takes away energy from work spot; it is more concerned in heat conductive material.
- It reduces the accuracy of micromachining operation due to heat diffusion away from the focal point, melts larger area, recasting of layers and collection of debris at surface.
- Area affected by heat diffusion results in micro/macro crack due to mechanical stress.
- It damages the nearby device structure or delaminate multilayer material.

V. ULTRA-FAST PULSE LASER MACHINING

The micromachining quality is a strong function of the amount of heat deposited in the work piece, or more exactly, a function of the amount of heat that is left behind in the material that can cause damage. Ultrafast pulses are extremely short (Femto second) and so short (\ll heat diffusion time) that the energy they deposit in material does not diffuse away from the micromachining spot. So much energy (intensity $\sim 100\text{TW}/\text{cm}^2$) is deposited in the material so fast that the material is forced into a state of matter called plasma. This plasma then expands away from the material as a highly energetic gas, taking almost all the heat away with it. The material goes from a solid to a gas phase without going through a melt phase. Consequently, very little heat is left behind to damage the material; so efficiency is high and due to plume droplet does not condense onto surrounding material. Thus machining quality is very good without melt zone, no cracks, no splattering of material etc. It is unique ability of ultrafast lasers to create this state (plasma) that is the reason why they produce results so different from those produced by traditional lasers as shown in Fig 1.

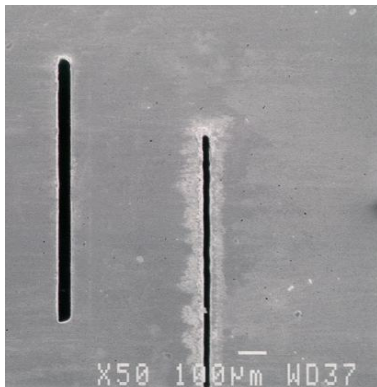


Fig 1: Sample machined with long pulse laser and ultra short pulse laser

VI. APPLICATIONS

Ultra short laser can be used for machining of hard material like diamond, tungsten and titanium with high aspect ratio (1:50). It can drill the hole at difficult angle (10deg). Excimer laser is used for drilling the nozzle hole- arrays for ink jet printer and μ -via/ via holes for high speed connection between surface mount components [5]. The laser micromachining is playing very critical role in biomedical like μ drills for analyzing arterial blood gases (ABG). Transparent material like glass does not absorb visible light - provided the intensity stays below the threshold for "multiphoton absorption" (via defect state or via inter-band absorption). Indeed, the multi-photon absorption process exhibits a highly non-linear dependence on the laser power density. When the intensity exceeds the threshold for plasma formation, much localized absorption does occur at the focal point spot. Once again, this plasma expands. But this time it is confined by the surrounding material. The effect of the expansion is to create a void within a very dense shell of material - a pit within the glass itself. This process is not limited to glass. Pits can be created in any material by focusing an ultrafast laser pulse inside the material, whether it is amorphous or crystalline.

VII. FABRICATION OF OPTICAL VIBRATION SENSOR

Single mode waveguide in glass materials can be fabricated with femtosecond lasers. At 775 nm, glass is transparent to incident light. Ultrafast laser pulses are used to locally melt the glass via confined multiphoton absorption and avalanche ionization inside the bulk material. The glass then resolidifies, changing its physical properties. The result is an index gradient that acts like a waveguide. A beam of light propagating along the same path in the glass will be guided in the same manner as an index-guided fiber guides light inside it. In [4], authors fabricated an optical vibration sensor using a high-repetition rate femtosecond laser

oscillator. The sensor consists of a single straight waveguide written across a series of three pieces of glass. The central piece is mounted on a suspended beam to make it sensitive to mechanical vibration, acceleration, or external forces. Displacement of the central piece is detected by measuring the change in optical transmission through the waveguide. The resulting sensor is small, simple, and requires no alignment. The sensor has a linear response over the frequency range 20 Hz–2 kHz, can detect accelerations as small as 0.01 m/s^2 , and is nearly temperature independent is shown in Fig 2.

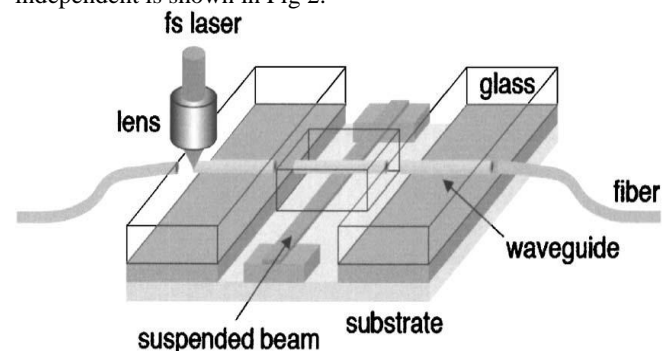


Fig 2: optical vibration sensor

VIII. CONCLUSION

Ultrafast laser pulses can machine materials (and/or locally change their chemical or physical properties) to produce no contamination to the surrounding material, no melt zone, no micro cracks, no shock wave, no delamination, no recast layer, and do damage to adjacent structures. It is highly reproducible, it can be used to create sub-micron features, and it can machine features inside transparent materials. Ultra fast lasers can micro machine virtually anything from metals to crystals to glass, ceramics and Teflon.

REFERENCES

- [1] R. Srinivasan, V. Mayne Banton, "Self-developing photoetching of poly (ethylene terephthalate) films by far ultraviolet excimer laser radiation", *Appl. Phys. Lett.* 41 (6), 1982.
- [2] Tsuneo Kuritaa, Kazuhisa Komatsuzakib, Mitsuro Hattori, "Advanced material processing with nano- and femto-second pulsed laser", *International Journal of Machine Tools & Manufacture*, 48, 2008, 220-227.
- [3] Deepa Bhatt, Karen Williams, David A. Hutt, Paul P. Conway, "Excimer Laser Micromachining of Glass Substrates", *OSA/CLEO/QELS*, 2008.
- [4] Masanao Kamata, Minoru Obaraa, "Optical vibration sensor fabricated by femtosecond laser micromachining", *Appl. Phys. Lett.* 87, 051106, 2005.
- [5] Malcolm C. Gower, "Industrial applications of laser micro machining", *Optics Express*, 7 (2), 2000, 56-67.

Simulation Based Performance Comparison of Adhoc Routing Protocols

Kushagra Agrawal*, Shaveta Jain**

*Department of Computer Science, Maharishi Markandeshwar University, Mullana, Ambala
agrawal_kushagra@rediffmail.com

** Department of Computer Science, Maharishi Markandeshwar University, Mullana, Ambala
shavetaj120@gmail.com

ABSTRACT

Ad Hoc network is a collection of wireless mobile hosts forming a temporary network without the aid of any centralized administration, in which individual nodes cooperate by forwarding packets to each other to allow nodes to communicate beyond direct wireless transmission range. Routing protocols of Mobile Ad-Hoc Network (MANET) use different approaches from existing Internet protocols because of dynamic topology, mobile host, distributed environment, less bandwidth, and less battery power. Adhoc routing protocols can be divided into two categories: table-driven (proactive schemes) and on-demand routing (reactive scheme) based on when and how the routes are discovered. In this paper, MANET routing protocols DSDV, AODV and DSR are compared using network simulator NS-2.34.

Keywords- MANET, Routing Protocols, AODV, DSR, DSDV and Throughput.

I. INTRODUCTION

Wireless network has become very popular in the computing industry. Wireless network are adapted to enable mobility. There exist three types of mobile wireless networks: Infrastructure Based Networks, Ad-Hoc Networks and Hybrid Networks. Fig 1 shows an Infrastructure Based Network that consists of wireless mobile nodes and one or more bridges, which connect the wireless network to the wired network. These bridges are called Base Stations (BS). A mobile node within the network searches for the nearest BS (e.g. the one with the best signal strength), connects and communicates with it. The important fact is that all communication is taking place between the wireless node and the base station but not between different wireless nodes.



Fig 1: An Infrastructure Based Network with Two Base Stations

On the other hand, the mobile node travels around and all of a sudden gets out of range of the BS, a handover to a new BS will let the mobile node communicate seamlessly with the new BS. In contrary

to Infrastructure Based Networks, an Ad-Hoc Network lacks any infrastructure. There are no BSs, no fixed routers and no centralized administration as shown in Fig 2. Mobile Ad-Hoc Network is an infrastructure-less network because all the mobile nodes work as routers. Each node forwards the packets unrelated to its own use [1] [2] [3].



Fig 2: A Mobile Ad-Hoc Network

All nodes move randomly and connected dynamically to each other. Therefore, all the nodes operate as a router and need to discover and maintain routes between source and destination in the network and to propagate packets accordingly. MANETs may be used in the areas with little or no communication infrastructure like emergency searches, rescue operations or places, where people wish to quickly share information.

II. ADHOC ROUTING PROTOCOLS

A routing protocol is needed whenever a packet needs to be transmitted to a destination via number of nodes. Numerous routing protocols have

been proposed for such kind of ad-hoc networks. These protocols find a route for packet delivery and deliver packet to the right destination. Basically, routing protocols can be broadly classified into three types as A) Table-Driven (Proactive Routing) Protocols, B) On-Demand (Reactive Routing) Protocols, C) Hybrid Routing Protocols as shown in Fig 3.

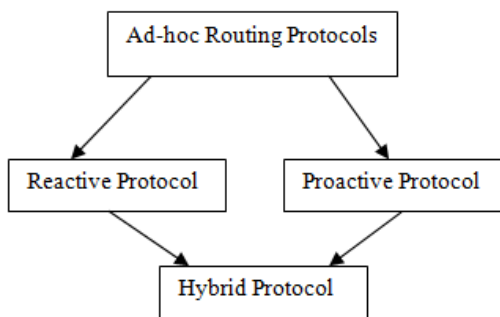


Fig 3: Types of Routing Protocols

2.1 Table-Driven (Proactive Routing) Protocols:

Every node maintains the network topology information in the form of routing tables by periodically exchanging routing information. Routing information is generally flooded in the whole network whenever routing table of any node is updated. It runs an appropriate path-finding algorithm on the topology information it maintains. Some of the existing table-driven protocols are DSDV, WRP, CGSR, OLSR, STAR, FSR, and GSR.

A.) Destination Sequenced Distance Vector (DSDV) Routing Algorithm- DSDV is a traditional table-driven protocol for MANET [4] based on the classical Bellman-Ford routing mechanism [5]. The improvements made to the Bellman-Ford algorithm include freedom from loops in routing tables. DSDV guarantees loop free paths at all instants. In proactive protocols, routes to all the nodes in the network are discovered in advance. Each node maintains a routing table, which contains entries for all the nodes in the network. Each entry consists of:

- the destination's address
- the number of hops required reaching the destination (hop count)
- the sequence number as stamped by the destination

Table maintained by all the nodes are broadcast after a fixed interval of time independent of any route changes or not. This increases the overhead and so decreases the throughput of network using DSDV protocol [12] [13] [14] [15].

The sequence numbers enable the mobile nodes to distinguish stale routes from new ones, thereby avoiding the formation of routing loops. Routing table

updates are periodically transmitted throughout the networking order to maintain table consistency. The routing updates can be “Event Driven” or “Time Driven”. These routing table updates can be sent via “full dump” or “incremental updates”. In incremental updates, only that information’s are sent which has change since last updates. Full Dump means sending whole routing table [16]. This type of packet carries all available routing information and can require multiple network protocol data units (NPDUs). During periods of occasional movement, these packets are transmitted infrequently. Smaller incremental packets are used to relay only that information which has changed since the last full dump. Each of these broadcasts should fit into a standard-size NPDU, thereby decreasing the amount of traffic generated. The mobile nodes maintain an additional table where they store the data sent in the incremental routing information packets. New route broadcasts contain the address of the destination, the number of hops to reach the destination, the sequence number of the information received regarding the destination, as well as a new sequence number unique to the broadcast [6]. The route labeled with the most recent sequence number is always used. In the event that two updates have the same sequence number, the route with the smaller metric is used in order to optimize (shorten) the path.

2.2 On-Demand (Reactive Routing) Protocols:

Protocols that fall under this category do not maintain the network topology information. They obtain the necessary path when it is required, by using a connection establishment process. Hence these protocols do not exchange routing information periodically. Some of the existing routing protocols that belong to this category are DSR, AODV, and TORA.

A.) Ad-Hoc On-Demand Distance Vector (AODV) Routing:

The AODV protocol is an improvement of the DSDV [7]. DSDV has its efficiency in creating smaller ad-hoc networks. Since it requires periodic advertisement and global dissemination of connectivity information for correct operation, it leads to frequent system-wide broadcasts. Therefore the size of DSDV ad-hoc networks is strongly limited. When using DSDV, every mobile node also needs to maintain a complete list of routes for each destination within the mobile network. The advantage of AODV is that it tries to minimize the number of required broadcasts. It creates the routes on a on-demand basis, as opposed to maintain a complete list of routes for each destination. Therefore, the authors of AODV classify it as a pure on-demand route acquisition system [8].

Path Discovery Process

When trying to send a message to a destination node without knowing an active route [9] to it, the sending node will initiate a path discovery process. A route request message (RREQ) is broadcasted to all neighbors, which continue to broadcast the message to their neighbors and so on. The forwarding process is continued until the destination node is reached or until an intermediate node knows a route to the destination that is new enough. To ensure loop-free and most recent route information, every node maintains two counters: sequence number and broadcast_id. The broadcast_id and the address of the source node uniquely identify a RREQ message. broadcast_id is incremented for every RREQ the source node initiates. An intermediate node can receive multiple copies of the same route request broadcast from various neighbors. In this case –if a node has already received a RREQ with the same source address and broadcast_id – it will discard the packet without broadcasting it furthermore. When an intermediate node forwards the RREQ message, it records the address of the neighbor from which it received the first copy of the broadcast packet. This way, the reverse path from all nodes back to the source is being built automatically. The RREQ packet contains two sequence numbers: the source sequence number and the last destination sequence number known to the source. The source sequence number is used to maintain “freshness” information about the reverse route to the source while the destination sequence number specifies what actually a route to the destination must have before it is accepted by the source [8].

When the route request broadcast reaches the destination or an intermediate node with a fresh enough route, the node responds by sending a unicast route reply packet (RREP) back to the node from which it received the RREQ. So actually the packet is sent back reverse the path built during broadcast forwarding. A route is considered fresh enough, if the intermediate node’s route to the destination node has a destination sequence number which is equal or greater than the one contained in the RREQ packet as shown in Fig 4. As the RREP is sent back to the source, every intermediate node along this path adds a forward route entry to its routing table. The forward route is set active for some time indicated by a route timer entry [10]. If the route is no longer used, it will be deleted after the specified amount of time. Since the RREP packet is always sent back the reverse path established by the routing request, AODV only supports symmetric links.

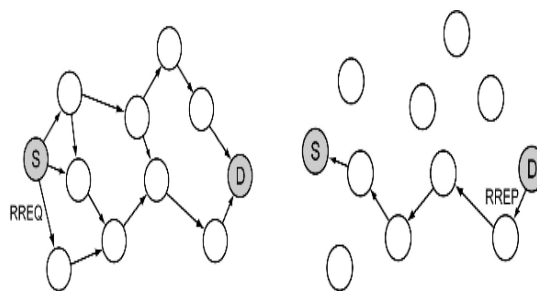


Fig 4: AODV Path Discovery Process

Maintaining Routes

If the source node moves, it is able to send a new RREQ packet to find a new route to the destination. If an intermediate node along the forward path moves, its upstream neighbor notices the move and sends a link failure notification message to each of its active upstream neighbors to inform them of the erasure of that part of the route as shown in Fig. 5. The link failure notification is forwarded as long as the source node is not reached. After having learned about the failure, the source node may reinitiate the route discovery protocol. Optionally a mobile node may perform local connectivity maintenance by periodically broadcasting hello messages [8].

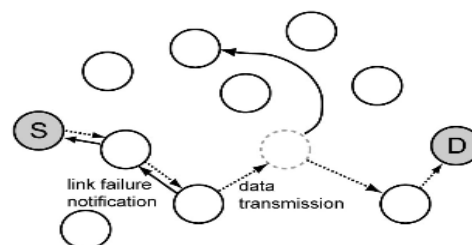


Fig 5: AODV Route Maintenance by Using Link Failure Notification Message

B.) Dynamic Source Routing (DSR): The DSR protocol is an on-demand routing protocol based on source routing. In the source routing technique, a sender determines the exact sequence of nodes through which to propagate a packet.

The list of intermediate nodes for routing is explicitly contained in the packet’s header. In DSR, every mobile node in the network needs to maintain a route cache where it caches source routes that it has learned. When a host wants to send a packet to some other host, it first checks its route cache for a source route to the destination. In the case a route is found, the sender uses this route to propagate the packet. Otherwise the source node initiates the route discovery process. Route discovery and route maintenance are the two major parts of the DSR protocol.

Route Discovery

For route discovery, the source node starts by broadcasting a route request packet that can be received by all neighbor nodes within its wireless transmission range. The route request contains the address of the destination host, referred to as the target of the route discovery [11], the source's address, a route record field and a unique identification number. At the end, the source host should receive a route reply packet containing a list of network nodes through which it should propagate the packets, supposed the route discovery process was successful. During the route discovery process, the route record field is used to accumulate the sequence of hops already taken as shown in Fig 6. First of all the sender initiates the route record as a list with a single element containing itself. The next neighbor node appends itself to the list and so on. Each route request packet also contains a unique identification number called request_id. request_id is a simple counter which is increased whenever a new route request packet is being sent by the source node. So every route request packet can be uniquely identified through its initiator's address and request_id. When a host receives a route request packet, it is important to process the request in the order as described below:

1. If the pair <source node address, request_id> is found in the list of recent route requests, the packet is discarded.
2. If the host's address is already listed in the request's route record, the packet is also discarded. This ensures removal of later copies of the same request that arrive by using a loop.
3. If the destination address in the route request matches the host's address, the route record field contains the route by which the request reached this host from the source node. A route reply packet is sent back to the source node containing a copy of this route.
4. Otherwise, add this host's address to the route record field of the route request packet and rebroadcast the packet.

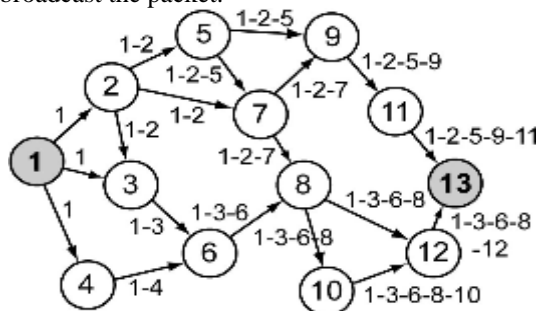


Fig 6: Building of the Route Record

A route reply is sent back either if the request packet reaches the destination node itself, or if the request

reaches an intermediate node which has an active route [10] to the destination in its route cache. The route record field in the request packet indicates which sequence of hops was taken.

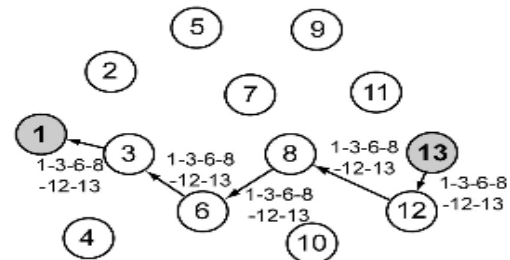


Fig 7: Propagation of the Route Reply

If the node generating the route reply is the destination node, it just takes the route record field of the route request and puts it into the route reply. If the responding node is an intermediate node, it appends the cached route to the route record and then generates the route reply as shown in Fig 7. If the responding node is an intermediate node, it appends the cached route to the route record and then generates the route reply. Sending back route replies can be accomplished in two different manners: DSR may use sym-metric links, but it is not required to. In the case of symmetric links, the node generating the route reply just uses the reverse route of the route record. When using unidirectional (asymmetric) links, the node needs to initiate its own route discovery process and piggyback the route reply on the new route request.

Route Maintenance

Route maintenance can be accomplished by two different processes:

- Hop-by-hop acknowledgement at the data link layer
- End-to-end acknowledgements

Hop-by-hop acknowledgement at the data link layer allows an early detection and retransmission of lost or corrupt packets. If the data link layer determines a fatal transmission error (for example, because the maximum number of retransmissions is exceeded), a route error packet is being sent back to the sender of the packet. The route error packet contains two parts of information: The address of the node detecting the error and the host's address which it was trying to transmit the packet to. Whenever a node receives a route error packet, the hop in error is removed from the route cache and all routes containing this hop are truncated at that point. End-to-end acknowledgement may be used, if wireless transmission between two hosts does not work equally well in both directions. As long as a route exists by which the two end hosts are able to communicate, route maintenance is possible. There may be different routes in both directions. In this case, replies or acknowledgements

on the application or transport layer may be used to indicate the status of the route from one host to the other. However, with end-to-end acknowledgement it is not possible to find out the hop which has been in error.

2.3 Hybrid Routing Protocol: Protocols belong to this category combine the best features of the above two categories. Nodes within a certain distance from the node concerned or within a particular geographical region are said to be within the routing zone of the given node. For routing within this zone a table-driven approach is used and for the nodes that are located beyond this zone an on-demand approach is used. Some of the protocols in this category are CEDAR, ZRP, and ZHLS.

III. PERFORMANCE ANALYSIS

NS2.34 is the simulator used for simulating the three routing protocols. NS2 is a Network Simulator which is used to simulate all type of networks and can be easily understandable by anyone. The following one quantitative performance metric is used for this study.

Throughput-The ratio of the total amount of data that reaches a receiver from a sender to the time it takes for the receiver to get the last packet is referred to as throughput. It is expressed in bits per second or packets per second. Factors that affect throughput in MANETs include frequent topology changes, unreliable communication, limited bandwidth and limited energy. A high throughput network is desirable.

$$\text{Throughput} = \frac{\text{no. of packets delivered}}{\text{unit time}}$$

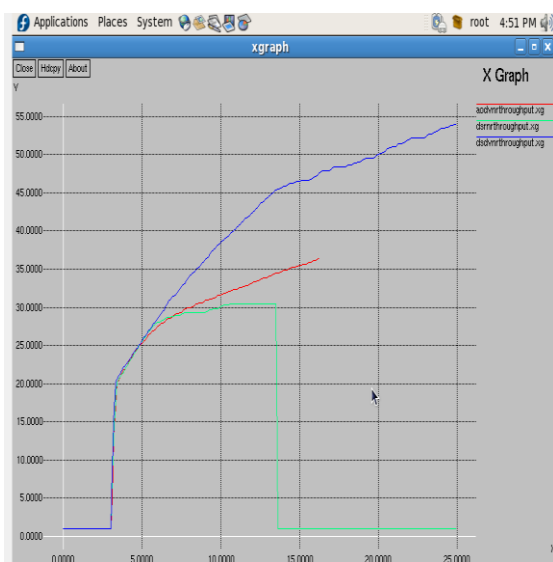


Fig 8: Throughput of AODV, DSR, DSDV Routing Protocol for 25 Nodes



Fig 9: Throughput of AODV, DSDV DSR Routing Protocol for 40 Nodes



Fig 10: Throughput of AODV, DSDV, DSR Routing Protocols for 100 Nodes

Fig 8 shows that the throughput of DSDV decrease for limited number of nodes. But as the number of nodes increases the throughput value of DSDV increases as shown in Fig 9 and Fig 10. DSDV is a proactive routing protocol and suitable for large number of nodes with low mobility due to the storage of routing information in the routing table 1 at each node.

Table 1: Simulation Parameters

PARAMETER	VALUE
Traffic Type	TCPNewreno
Number of Nodes	25,40 and 100
Area Covered	1000 X 1000
Routing Protocols	AODV, DSDV and DSR
Simulation Time	25ms

IV. CONCLUSION

Routing protocol DSDV uses proactive “table driven” routing, while AODV and DSR use reactive “on-demand” routing. Protocol DSDV periodically updates its routing tables, even in cases when network topology doesn’t change. AODV protocol has inefficient route maintenance, because it has to initiate a route discovery process every time network topology changes. Both protocols, AODV and DSR, use route discovery process, but with different routing mechanisms. In particular, AODV uses routing tables, one route per destination, and destination sequence numbers as a mechanism for determining freshness of routes and route loops prevention. On the other hand, DSR uses source routing and route caching, and doesn’t depend on any periodic or time-based operations.

The performance of the three Routing protocols was analyzed using NS-2 Simulator. When comparing the routing throughput by each of the protocols, DSDV has the high throughput. It measures of effectiveness of a routing protocol. The throughput values of DSDV, AODV and DSR Protocols for 25, 40 and 100 Nodes. Based on the simulation results, the throughput value of AODV slowly increases initially and maintains its value when the time increases. AODV performs well than DSR since AODV is an on-demand protocol. The throughput value of DSR increases at lower pause time and grows as the time increases. Hence, DSDV shows better performance with respect to throughput among these three protocols.

V. FUTURE WORK

A comparison of routing protocols AODV, DSR and DSDV has been carried out. It is proposed to compare all other routing protocols considering the same simulation parameters so that an exhaustive comparison of various routing protocols can be made. Also, it would be interesting to observe the behavior of these protocols by varying other network parameters like Simulation time, Simulation areas, Traffic type etc. More performance metrics can also be considered. These protocols can also be compared with their existence & the work presented here can be used as a reference for future.

REFERENCES

- [1] Bulent Tavli, “Mobile Ad Hoc Networks: Energy-Efficient Real-Time Data Communications”, CRC Press, 2006.
- [2] Azzedine Boukerche, “Algorithms and Protocols for Wireless, Mobile Ad Hoc Networks”, 2008.
- [3] Mohammad Ilyas, Richard C. Dorf, “The handbook of ad hoc wireless networks”, 2003.
- [4] Charles E. Perkins, “Ad Hoc Networking”, Addison Wesley, 2001.
- [5] C. E. Perkins and E. M. Royer, “Ad-hoc on demand distance vector routing,” in Proceedings of the 2nd IEEE Workshop on Mobile Computing Systems and Applications (WMCSA’99), New Orleans, LA, USA, February 1999, 1-11.
- [6] C. E. Perkins and P. Bhagwat, “Highly Dynamic Destination-Sequenced Distance-Vector Routing (DSDV) for Mobile Computers”, *Comp. Commun. Rev.*, 1994, 1-11.
- [7] T. Camp, J. Boleng, and V. Davies, “A survey of mobility models for ad hoc network research”, *Wireless Communications and Mobile Computing (WCMC): Special issue on Mobile Ad Hoc Networking: Research, Trends and Applications*, 2002, 1-26.
- [8] C. E. Perkins and E. M. Royer, “Ad-hoc on demand distance vector routing”, *Proceedings of the 2nd IEEE Workshop on Mobile Computing Systems and Applications (WMCSA’99)*, 2(9), 1999, 727-732.
- [9] C. Perkins and P. Bhagwat, “Highly dynamic destination-sequenced distance-vector routing (DSDV) for mobile computers”, *Proceedings of the ACM SIGCOMM’94-Conference on Communications Architectures, Protocols and Applications*, 1999, 234-244.
- [10] C. Perkins, E. Belding-Royer, and S. Das, “RFC 3561: Ad hoc on-demand distance vector (AODV) routing”, Available at: <ftp://ftp.isi.edu/in-notes/rfc3561.txt>, 2003.
- [11] D. B. Johnson and D. A. Maltz, “Dynamic source routing in ad hoc wireless networks,” in *Mobile Computing*, T. Imielinski and H. Korth, Eds. Kluwer Academic Publishers, 1996, 1-25.
- [12] Josh Broch, David A. Maltz, David B. Johnson, Yih-Chun Hu, Jorjeta Jetcheva, “A Performance Comparison of Multi-Hop Wireless Ad Hoc Network Routing Protocols”, 1994, 1-13.
- [13] Tony Larson, Nicklas Hedman “Routing Protocols in Wireless Ad-hoc networks- A simulation Study”, 1998.
- [14] Azzedine Boukerche, “Algorithms and Protocols for Wireless, Mobile Ad Hoc Networks”, ISBN: 978-0-470-38358-2, 2008, Wiley-IEEE Press.
- [15] Nadia Qasim, Fatin Said, Hamid Aghvami, “Mobile Ad Hoc Networks Simulations Using Routing Protocols for Performance Comparisons”, *Proceedings of the World Congress on Engineering*, London, U.K., 1(1), 2008, 24-32.
- [16] Asma Tuteja, Sunil Thalia, Rajneesh Gujral, “Comparative Performance Analysis of DSDV, AODV and DSR Routing Protocols in MANET using NS2” in *ACE (Advances in Computer Engineering) 2010*, an IEEE Conference held from 21 - 22 June at Bangalore, India, ISBN No. 978-1-4244-7154-6, 330-333.

matching, nearest neighbor indexing, clustering, and solutions for affine parameters [3].

II. APPLICATIONS OF OBJECT DETECTION

There are various applications of object detection used in real world. Some of them are given as follows:

- (a) Object Detection is also used to detect cracks in manufacturing companies.
- (b) Object detection is also used in vehicle number plate detection.
- (c) Face animation effects for the entertainment industry.
- (d) Video surveillance systems with automatic face identification.
- (e) Object detection has also application in the security purpose.
- (f) Used in digital camera image to detect the different images.
- (g) Object detection is used in medical line as an application to skin cancer screening.

III. TECHNIQUES USED FOR OBJECT DETECTION AND CRACK DETECTION

Some of the techniques used to detect objects in real world are Object Recognition with Hierarchical Kernel Descriptors, Depth Kernel Descriptors for Object Recognition, Real object recognition using moment invariants [11], Mining spatial related features for object recognition , SVM used in Segmentation as Selective Search for Object Recognition [6], Real-Time Human Pose Recognition from Depth Image, Fast Concurrent Object Localization and Recognition, Seam Carving and Saliency Map [7], technique based on mathematical Morphology and Correlation Coefficient [8], Using Stereo [9], Efficiently Combining Contour and Texture Cues for Object Recognition. Dataset consisting of segmented RGB and depth images are used. Each techniques have its own advantages and disadvantages and also having different applications. Brief explanations of some papers using various techniques are given below:

3.1 Probabilistic Categorization of Kitchen Objects:

In [12], authors presented a system that can extract features from different sensor modalities for solving the problem of classifying different objects present in kitchen environments as shown in Fig. 2 and Fig. 3. Authors used statistical relational learning methods (Markov Logic Networks and Bayesian Logic Networks) to capture complex interactions between the different feature spaces. To show the effectiveness of approach, proposed system is analyzed and validated for the problem of recognizing objects in table settings scenarios. The classification results

(Table 1), which indicate an overall classification rate of about 54%, yet the accuracy on properly segmented objects is almost 70%. The time taken for a run of the feature estimation and the classifier on a single scene was a few seconds.

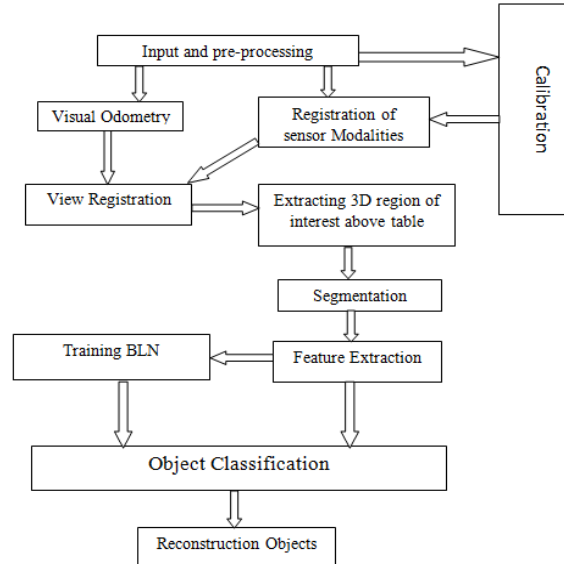


Fig 2: Probabilistic Categorization of Kitchen Objects

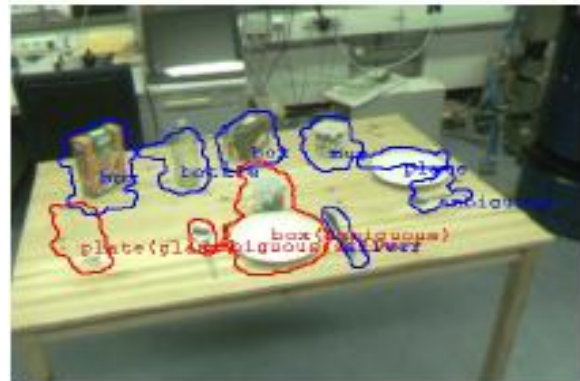


Fig 3: Correctly classified clusters are marked with blue, while incorrectly classified ones with red, and the ground truth is shown in parenthesis

Table 1: Table for Categorization Result

Class	Correct	Number	Ratio
1 - box	23	27	0.85
2 - plate	52	67	0.78
3 - glass	7	31	0.23
4 - mug	39	40	0.98
5 - bottle	4	5	0.80
6 - silver	21	43	0.57
7 - ambiguous	17	87	0.20
overall (1-7)	163	300	0.54
objects (1-6)	146	213	0.69

3.2 Depth Kernel Descriptors for Object Recognition:

Motivated by local descriptors on images, in particular kernel descriptors [2], authors developed a set of kernel features on depth images that model size, 3D shape, and depth edges in a single framework as shown in Fig. 4. Through extensive experiments on object recognition, author demonstrated that (1) local features capture different aspects of cues from a depth frame/view that complement one another; (2) kernel features significantly outperform traditional 3D features (e.g. Spin images); and (3) significantly improve the capabilities of depth and RGB-D (color + depth) recognition, achieving 10–15% improvement in accuracy over the state of the art. Authors proposed a range of local features over a depth image and showed that for object recognition they are superior to pose-invariant features like Spin Images.

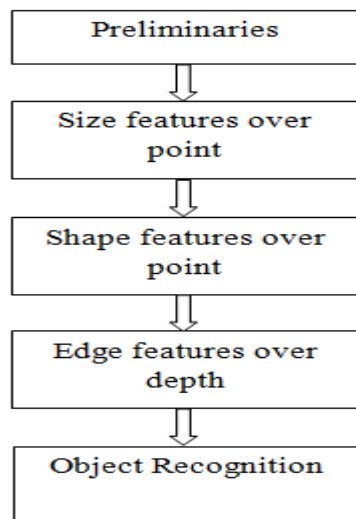


Fig 4: Flowchart for object detection using Depth Kernel Descriptors

Table 2: Accuracies of depth kernel descriptors on the RGB-D object dataset (in percentage)

Features	Instance	Category
Size KDES	32.0	60.0±3.3
KPCA	29.5	50.2±2.9
Spin KDES	28.8	64.4±3.1
Gradient KDES	39.8	69.0±2.3
LBP KDES	36.1	66.3±1.3
Combination	54.3	78.8±2.7

Table 2 shows the accuracy of depth kernel descriptors, where Size KDES means size kernel descriptors; KPCA means kernel PCA based shape features; Spin KDES means spin kernel descriptors; gradient KDES means gradient kernel descriptors;

LBP KDES means local binary pattern kernel descriptors. ± means standard deviation.

3.3 Mining Spatial Related Features:

High probability is that keypoints are related and reliable enough to give more weight when forming the feature vector. Their approach is important because only the most frequent and meaningful keypoints are included in the feature vector, while ignoring random and meaningless keypoints as shown in Fig. 5. Moreover, keypoints belonging to a spatial relationship will be given more weight than independent keypoints [1].

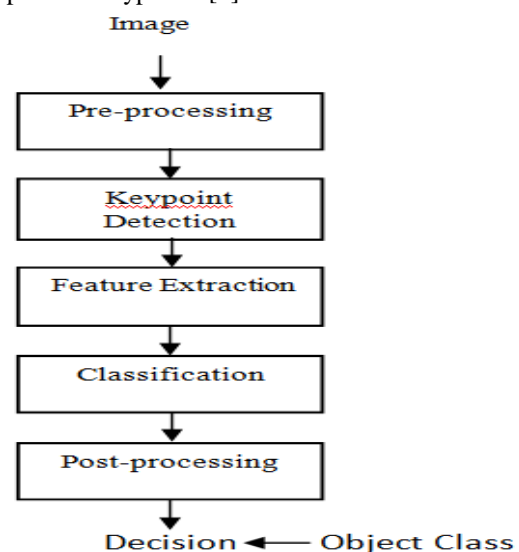


Fig 5: Flowchart for object detection by constructing feature vectors.

The approach [3] is appealing because we believe that a clear pattern can easily be learnt by using machine learning techniques (Fig. 6) if we provide a set of small but extremely meaningful attributes (keypoints features).

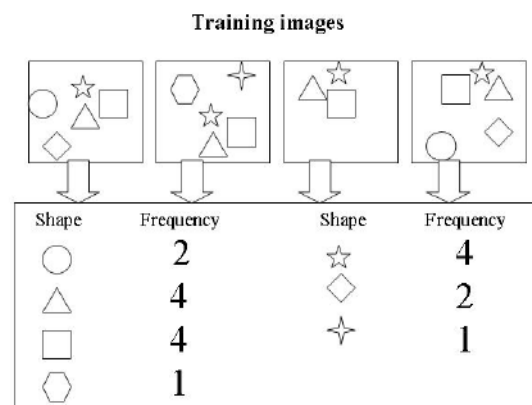


Fig 6: Extracting most frequent features

3.4 Object Recognition based on Mathematical Morphology and Correlation Coefficient:

A technique based on slicing the image to equally sub-areas, and then applying the density slicing to the colour histogram of these areas combined with the color pair technique and then shape recognition method is proposed [4] as a higher level phase in proposed system. This new approach may be categorized under the region-based methods for shape-based retrieval as shown in Fig. 7 and Fig. 8. The approach is capable of solving the most prominent drawback of using region-based methods that is the problems related to unrelated intensity edges to the boundary of the objects within the image as shown in Table 3. Use of Laplacian of Gaussian removes the unwanted intensity edges formulated through noise [4].

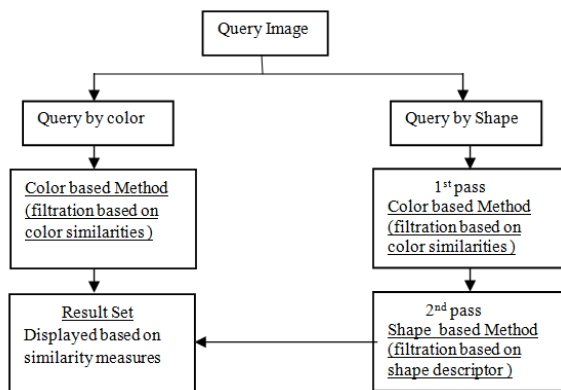


Fig 7: System Flow diagram for object recognition using shape feature extraction.

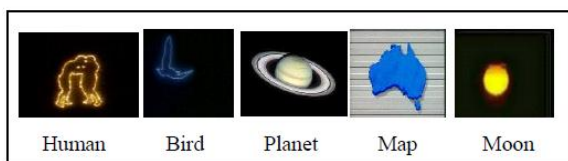


Fig.8: Sample images

Table 3: Execution time in seconds.

	Execution time in seconds		
	$r \geq 0.50$	$r \geq 0.80$	$R \geq 0.10$
Human	4.70	2.73	6.03
Bird	6.86	2.13	8.05
Planet	6.48	4.23	9.18
Map	3.42	1.89	4.08
Moon	5.05	3.57	7.41
Average	5.302	2.91	6.95

3.5 Automation of pavement surface crack detection using the continuous wavelet transform:

It presents a new approach in automation for crack detection on pavement surface images. The method is based on the continuous wavelet transform as shown in Fig. 9. In the first step, a separable 2D continuous wavelet transform for several scales is performed. Complex coefficient maps are built. The angle and modulus information are used to keep significant coefficients. Then, wavelet coefficients maximal values are searched and their propagation through scales is analyzed. Finally, a post-processing gives a binary image which indicates the presence or not of cracks on the pavement surface image. Consequently, author have chosen to work with images whose spatial resolution is between 1 and 2 mm per pixel [5].

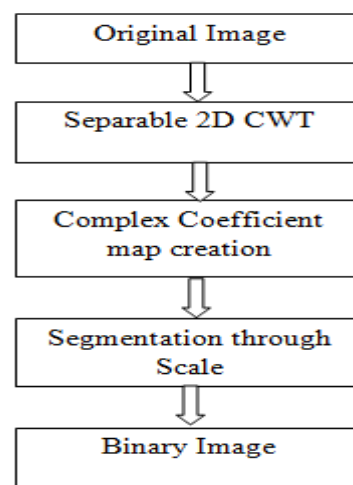


Fig 9: Flowchart of crack detection using continuous wavelet transforms.

IV. Conclusion:

With the help of different techniques, we can detect shape of different objects and cracks in real world. In this paper, we gave a comparison among different techniques used for object detection. Crack detections play important role to find the defects during manufacturing like in pipelines, in utensils and spare parts of machines and we can also able to find the cracks in roads, buildings and surface of earth during earthquakes . Object Detection is used to find the shape of object and to find th category of object. Depth Kernel considers the model size, 3D shape, and depth edges in a single framework of depth image. Construting feature vectors is used in mining spatial related features, bag-of-features technique is used in seam carving and saliency map, stereo method is also used for object recognition, shape feature extraction is used in object recognition based on mathematical morphology and correlation coefficient and SVM technique is used in segmentation as selective search for object recognition. We are trying to make a technique which will improve the efficiency and

accuracy of object Recognition and also detect the defective piece by detection of cracks or some damage in their shape.

Composite Sensor”, *The 2009 IEEE/RSJ International Conference on Intelligent Robots and Systems, 2009, 4777-4784.*

REFERENCES

- [1] Liefeng Bo ,Kevin Lai, Xiaofeng Ren, Dieter Fox, “Object Recognition with Hierarchical Kernel Descriptors”, *IEEE International Conference on Computer Vision and Pattern Recognition (CVPR), 2011, 1729-1736.*
- [2] L. Bo, X. Ren, and D. Fox. “Kernel Descriptors for Visual Recognition”, *In NIPS, 2010, 1-9.*
- [3] Edmond Zhang, “Mining Spatially Related Features for Object Recognition”, *NZCSRSC, 2008, 271-273.*
- [4] Muharrem Mercimek, Kayhan Gulez and Tarik Veli Mumcu, “Real object recognition using moment invariants”, *SADHANA, 30 (6), 2005, 765-775.*
- [5] Peggy Subirats, Jean Dumoulin, Vincent, Legeay and Dominique Barba, “Automation of pavement surface crack detection using the continuous wavelet transform”, *IEEE 1-4244-0481-9/06, 2006.*
- [6] Koen E. A. van de Sande, Jasper R. R. Uijlingsy-University of Amsterdam , Theo Gevers, Arnold, W. M. Smeulders, “Segmentation as Selective Search for Object Recognition”, *International Journal of Computer Vision, Volume 104 (2), 2013, 154-171.*
- [7] Motoaki Sato and Jiro Katto, “Performance important of generic object recognition by using seam carving and saliency map”, 2011.
- [8] Jehad Alnihoud, “An efficient region-based approach for object Recognition and retrieval based on mathematical Morphology and correlation coefficient”, *The International Journal of Information Technology, 5 (2), 2008.*
- [9] Scott Helmer and David Lowe, “Using Stereo for object Recognition”, *International Conference on Robotics and Automation (ICRA), Anchorage, Alaska, 2010.*
- [10] Lowe, David G., “Three-dimensional object recognition from single two-dimensional images,” *Artificial Intelligence, 313, 1987, 355-395.*
- [11] D. Lowe. “Distinctive image features from scale-invariant keypoints”. *IJCV, 60, 2004, 91-110.*
- [12] Zoltan-Csaba Marton, Radu Bogdan Rusu, Dominik Jain, Ulrich Klank, and Michael Beetz, “Probabilistic Categorization of Kitchen Objects in Table Settings with a

An Overview of PAPR Reduction Optimization Algorithm for MC-CDMA System

Kanchan Singla*, Rajbir Kaur, Gagandeep Kaur*****

* (Department of Electronics and Communication, Punjabi University, Patiala, India
Email: singlakanchan08@gmail.com)

** (Department of Electronics and Communication, Punjabi University, Patiala, India
Email: rajbir277@yahoo.co.in)

*** (Guru Nanak Institute of Technology, Mullana, Ambala, India
Email: gaganksodhi@gmail.com)

ABSTRACT

Multicarrier Code Division Multiple Access (MC-CDMA) has attracted lot of attention from researchers as it plays an important role in wireless communication. The challenging problem of MC-CDMA is high peak to average power ratio due to large number of sub-carriers which reduces the system performance. There are many PAPR reduction techniques for MC-CDMA. This paper focus on review of different optimization methods used for PAPR reduction. To reduce PAPR the restraints are low power consumption, and low Bit Error Rate (BER).

Keywords - Ant colony optimization, MC-CDMA, OFDM, Peak to average power ratio

I INTRODUCTION

Future wireless systems such as fourth generation (4G) cellular will need tractability to provide subscribers with a variety of services such as voice, data, images and video signal. Code division multiple accesses (CDMA) have shown very successful for large scale cellular voice systems, but there is some agnosticism about whether CDMA will be well-suited to non-voice traffic [1]. Multicarrier CDMA (MC-CDMA) has emerged as a powerful alternative to conventional direct sequence CDMA (DSSSS) in mobile wireless communications.

Multicarrier code division multiple access (MC-CDMA) is combination of code division multiple access (CDMA) and orthogonal frequency division multiplexing (OFDM). It is a very attractive wireless communication system. The MC-CDMA has advantages of both the CDMA and OFDM systems. MC CDMA technique achieve high data rate transmission with protection against both frequency selective fading and time dispersion channel while at the same time offers a spectrum efficient multiple access strategy [2]. In Multi-Carrier CDMA, the input data streams are split into several sub-streams in parallel, and then modulate several subcarriers with each sub-stream before transmitting signals.

Despite the advantages of the MCCDMA, one of the main drawbacks is high peak-to-average power ratio (PAPR), which causes bit-error-rate (BER), performance degradation of the system. The PAPR has disadvantages such as the design complexity of Analog to Digital Converter (ADC) and Digital to

Analog Converter (DAC). The high PAPR should be reduced to eliminate the non-linear distortion effect of the high-power amplifier (HPA) [3].

To reduce high PAPR, various techniques are proposed which are used for both OFDM and MC CDMA. These techniques are divided into three categories: signal distortion techniques, signal scrambling techniques and coding techniques. Signal distortion schemes include clipping, peak windowing, peak cancellation and companding. Scrambling scheme includes Selected Mapping (SLM), Partial Transmit Sequence (PTS). Coding techniques are used for signal scrambling, such as Golay complementary sequences, Shopire-Rudin sequences, and barker codes. To reduce high PAPR of MC CDMA, there are many optimization algorithm present like swarm optimization, which is basic of all other algorithms. Other algorithm are chip optimization, artificial ant colony optimization, genetic algorithm, artificial bee colony algorithm etc. In this paper we have described review of different algorithms.

This paper is organised as follow: in section 2, MC-CDMA system model, PAPR of MC CDMA are described. In section 3, various optimization algorithms such as artificial bee colony algorithm, chip interleaving and its optimization genetic algorithm, ant colony optimization are described. In section 4, the paper is concluded.

II SYSTEM DESCRIPTION

2.1 MC-CDMA System Model

In MC-CDMA model, there are K active users and for each kth user $d^{(k)} = [d_1^{(k)}, d_2^{(k)}, \dots, d_M^{(k)}]$ denotes the M modulated data symbols, where $k=1,2,\dots,K$. Modulated data symbols are converted into M parallel data streams. After this conversion each symbol is multiplexed by a user specific spreading code $c^{(k)} = [c_1^{(k)}, c_2^{(k)}, \dots, c_j^{(k)}]$, where j represents the spreading factor (SF) or spreading code. Data of multiple user's can be transmitted in same frequency space and at same time as the spreading codes have property of orthogonally as shown in Fig 1. In this, we use Walsh hadamard sequences as spreading sequences. The input of K user is added and interleaved in frequency domain as $X = [X_0, X_1, \dots, X_{N-1}]^T$, where N is number of sub carriers. After frequency interleaving, the interleaved symbols are input into the IFFT block of size $N=M \times J$. The resultant baseband signal for MC-CDMA is expressed as:

$$x(t) = \frac{1}{\sqrt{N}} \sum_{m=1}^M \sum_{j=1}^J \sum_{k=1}^K d_m^{(k)} c_j^{(k)} e^{j2\pi\{M(j-1)+(m-1)\}t/T_s} \quad (1)$$

Where, T_s is symbol period of signal, in which $0 \leq t \leq T_s$ [4].

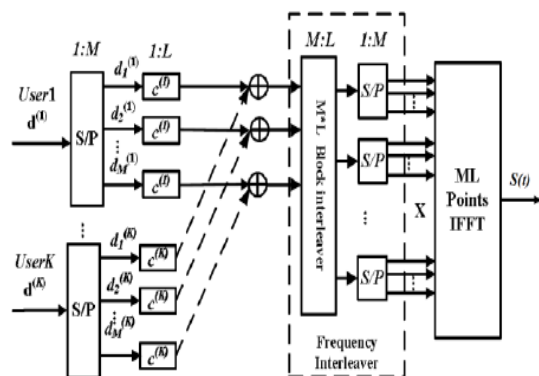


Fig 1: MC-CDMA transmitter model [4]

2.2 Peak To Average Power Ratio

Though MC-CDMA is a powerful multiple access technique but it is not problem free. The challenging problem of MC CDMA is high PAPR. In time domain, multicarrier signal is the result of addition of many narrowband signals. This addition is large at some time instances and small at other, it means that the peak value of the signal is larger than

the average value [5]. MC-CDMA has large number of independently modulated sub carriers and N modulated subcarriers are added with same phase. So peak power becomes N times the power of MC-CDMA signal. High PAPR values causes a serious problem to linear power amplifier (PA) used at transmitter.

PAPR of the MC-CDMA signal is the ratio of the peak power to the average power of a multicarrier signal. It is represented as:

$$\text{PAPR} = \frac{P_{peak}}{P_{average}} = 10 \log_{10} \frac{\max \left\{ \left| \sum_{k=1}^K d_k e^{j\omega_k t} \right|^2 \right\}}{E \left\{ \left| \sum_{k=1}^K d_k e^{j\omega_k t} \right|^2 \right\}} \quad (2)$$

where P_{peak} is output peak power and $P_{average}$ is output average power.

III PAPR REDUCTION OPTIMIZATION ALGORITHM

3.1 Artificial Bee Colony Algorithm

The ABC algorithm is a swarm-based optimization algorithm, which simulates intelligent foraging behavior of a honeybee swarm. In this, the position of a food source gives a possible solution to the optimization problem and quantity of nectar in the food source corresponds to quality (fitness) of the associated solution. Foraging bees are classified into three phases, employed, onlookers and scouts. At initial phase, the ABC yields a randomly distributed population with employed bees. An employed bee generates a modification of position (solution) in her memory, depending on the local information (visual information), and investigates the nectar amount (fitness value) of the new source. If amount of new nectar is higher than the previous source, the bee memories the new position and forgets the old one. Otherwise, bee memories the position of the previous source in her memory.

After all employed bees finish this search process, they share the nectar information about food sources and their position information with the onlooker bees. An onlooker bee judges the nectar information taken from the employed bees and prefers the food source with probability related to its nectar amount. Like the employed bee, the onlooker bees make a modification of the position in her memory and examine the nectar amount of the potential source. If amount of nectar is higher than that of the previous source, the bee memories the new position and forgets the old one.

After the completion of searches of onlooker bees, scouts are determined. The employed bee of an exhausted source becomes a scout and begins to search randomly for a new food source. These steps are repeated through a number of cycles, called

maximum number of cycles, or until a termination standard is satisfied. The main steps of the ABC algorithm are:

- Initialize the population
- Repeat
- Place the employed bees on their food sources
- Place the onlooker bees on the food sources depending on their nectar amounts
- Send the scouts bees to the search area for discovering new food sources
- Memories the best food source solution achieved so far
- until requirements are met [6].

3.2 Chip Interleaving and Optimization

This reduction technique is used for uplink in M-modification in MC-CDMA system. In M-modification, total number of subcarriers N_C is divided into m groups having L sub-carriers in each. For one user (uplink) every group of L subcarriers transmits one symbol spread with sequence of length L . The user transmits M parallel data symbols on all sub-carriers. Walsh sequences are used for spreading in this case and introduce some kind of redundancy to the system. For example sequence 1-1 1 will continue with -1. OFDM based systems (MC-CDMA included) are presented in time domain by addition of sinusoids. The peak value of addition of sinusoids (representing chip sequences) is reduced by changing the position of chip. When no chip interleaving is used, the first chip is on first sub-carrier, second chip on the second sub-carrier, etc. This can be symbolized by vector [1 2 3 4 5... N_C]. The permutation of vector, for example [3 6 9 13 ...], symbolized the chip interleaving pattern where the first chip is modulated on third sub-carrier, second chip on the sixth sub-carrier and so on.

The principle of this access is to find the interleaving pattern which minimizes PAPR. The chip interleaving pattern must be same for all users in the system to keep orthogonal among them, Number of possible interleaving pattern stands with the number of sub-carriers in system which makes direct search algorithm improper for the system with more sub-carriers. So, optimum searching algorithms such as Genetic Algorithm (GA) and Ant Colony Algorithm (ACA) are used to solve this problem [7] [8].

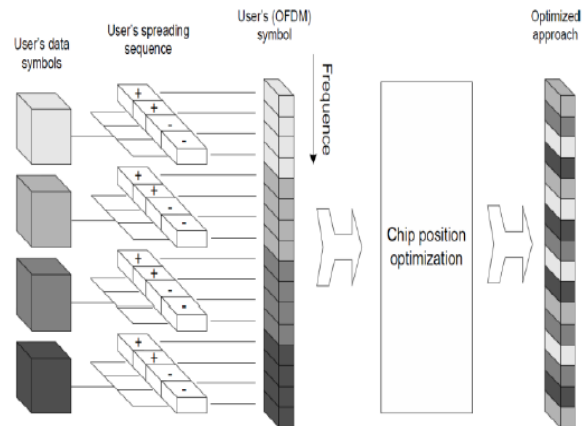


Fig 2: M- Modification of MC CDMA and its optimization [7]

3.3 Genetic Algorithm

Genetic optimization is based on the technique known as swarm intelligence, which is a part of artificial intelligence. The GA use combination of previous best solutions to obtain better one. This algorithm starts with random set of solutions called population. In every step (generation) new population is created from the old one. New individuals are made from old ones (parents). The probability for an individual becoming the parent depends upon its fitness function. The variation is introduced to prevent falling in local optimum.

Permutation encoding is used for implementing of chip spreading. In permutation encoding, each individual is represented by string of numbers (1.....48) that represents the position in a sequence. The fitness function (mean PAPR of that sequence for all possible data) is measured for each individual. The parent selection is made on random selection of 3 individuals and finds the best of them (according to fitness) which became parent. Crossover is created by one crossover point selection and permutation is copied from first parent till the crossover point and rest is from second parent. After that, the duplications of numbers must be interchanged by unused ones. The variation is made by simple swap of two numbers; one variation in one generation is presented. The best solution in the current generation is called elite and it is replicate in the next generation without differences (until better one is founded) [9]. Fig. 3 describes the value of fitness function in particular generations.

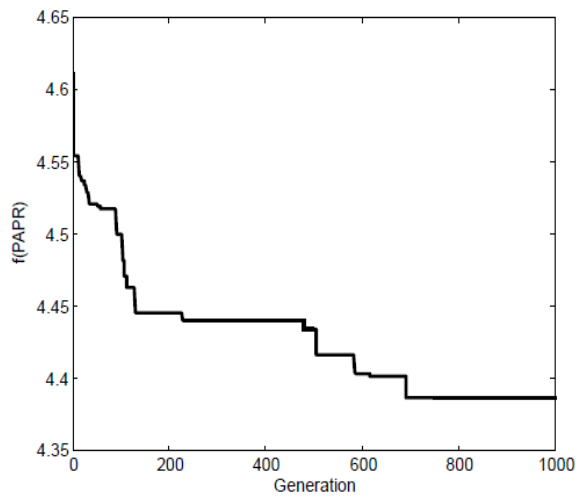


Fig 3: GA optimization process [9]

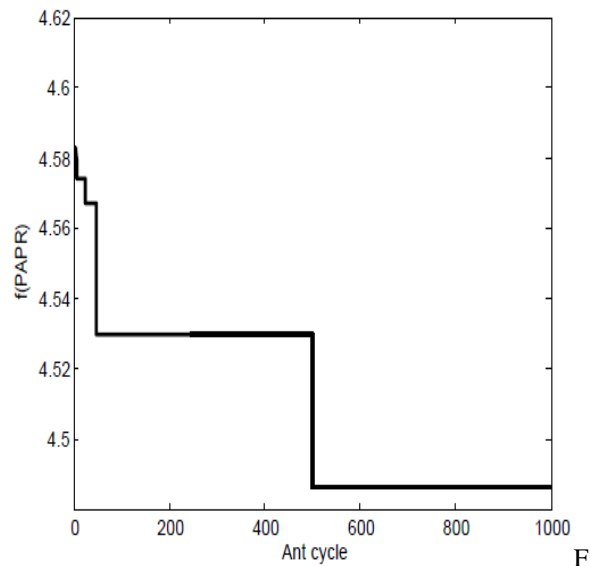


Fig 4: ACO Process [9]

3.4 Ant Colony Optimization

Ant Colony Optimization (ACO) is a metaheuristic approach for solving hard combinatorial optimization problems [10]. This technique represents distributed solution of difficult problems by lots of locally interacting simple agents called ants. They travel by sections called towns to make complete way with all towns. Each ant left trail on its way. The intensity of trail depends upon PAPR of sequence built by the ant. The ant makes decision which town will be visited next depending on trail laid on the way to towns. This makes the positive feedback in the algorithm. The pheromone trail act as communication medium between real ants. The pheromone trails in ACO service as distributed, numerical information which the ants use to probabilistically make solutions to the problem being solved. The PAPR of sequence is evaluated only after complete tour of ants, so trial is computed only ones in complete cycle.

The trail intensity is updated after complete cycle according to:

$$T_{ij} \left(\leftarrow +1 \right) \leftarrow Q \cdot T_{ij} \left(\leftarrow \right) + \Delta T_{ij} \quad (3)$$

where Q is coefficient such that $(1 - Q)$ represents evaporation of trail. The ΔT_{ij} is tray intensity increment on edge (i, j) (between towns i and j) obtained as:

$$\Delta T_{ij} = \sum_{k=1}^m \Delta T_{ij}^k \quad (4)$$

Where ΔT_{ij} is the quantity of trail substance [9]. The running of algorithms is visualized as function of best solution (elite) according to Cycle in Fig.4.

IV CONCLUSION

In this paper, we have presented different optimization algorithm for PAPR reduction which is challenging problem in MC CDMA. Although Chip interleaving has advantages of low complexity, no performance degradation, no side information but worst case of PAPR is still present. ABC algorithm has low computational complexity and less computational time. GA is slightly better and has less computation time. ACO is better among all as it reduces the probability of having PAPR value. Besides this, ACO has small complexity and no side information.

REFERENCES

- [1] A. Mahat, G. Sable, "An overview: performance improving techniques of mc-cdma", *Journal of Information, Knowledge and Research in Electronics and Communication*, 2 (2), 2013, 864-865.
- [2] S. Hara, R. Prasad, "Overview of Multicarrier CDMA", *IEEE Commun. Mag.*, 35 (12), 1997, 126 – 133.
- [3] B. Sarala, D. S. Venkateswarulu, B. N. Bhandari, "Overview of MC CDMA PAPR Reduction Techniques", *International Journal of Distributed and Parallel Systems*, 3 (2), 2012, 193-206.
- [4] G. Kaur, R. Kaur, "PAPR Reduction of an MC-CDMA System through PTS Technique using Suboptimal Combination Algorithm", *International Journal of Engineering Research and Applications (IJERA)*, 2 (4), 2012, 1192-1196.

- [5] G. Kaur, R. Kaur, Comparative study of SLM and PTS techniques for PAPR Reduction of an MC-CDMA system, *International Journal of Engineering Research and Applications (IJERA)*, 2 (4), 201, 779-784.
- [6] N. Taspınar, D. Karaboga, M. Yildırım, B. Akay, “Partial transmit sequences based on artificial bee colony algorithm for peak to average power ratio reduction in multicarrier code division multiple access systems”, *IET Commun.*, 5(8), 1155–1162.
- [7] G. Kaur, R. Kaur, An Overview of PAPR Reduction Techniques for an MC-CDMA System, *International Journal of Advanced Research in Computer Engineering & Technology*, 1 (4), 2012.
- [8] Z. Fedra, R. Marsalek, V. Sebesta, Chip “Interleaving and its Optimization for PAPR Reduction in MC-CDMA”, *Radio engineering*, 16 (4), 2007, 19-23.
- [9] Z. Fedra, V. Sebest, “Genetic algorithm and ant colony optimization for PAPR reduction in MC-CDMA”, *Radio elektronika 2006, Bratislava (Slovak Republic)*, 2006, 1-4.
- [10] U. Jaiswal, S. Aggarwal, “Ant Colony Optimization”, *International Journal of Scientific & Engineering Research*, 2 (7), 2011, 1-7.

A Review on Photoelectrochemical Splitting of Water by Semiconductors

P.K. Farsoiya*, D. Prasad A.*

*(Department of Chemical engineering and Technology, IIT BHU, Varanasi-221005
Email: farsoiya@gmail.com)

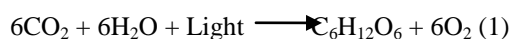
ABSTRACT

Hydrogen, if it can be produced using solar energy, stored and transported safely then it has the potential to be a non-fossil fuel. Research and development of an efficient system for solar energy to hydrogen energy is one of the challenging tasks to solve global energy problem. This article will give a short review on photoelectrochemical approaches for water splitting using semiconductor anodes.

Keywords – Hydrogen, Photoelectrochemistry, Photoelectrolysis, Semiconductor, Solar Energy, Water splitting

I INTRODUCTION

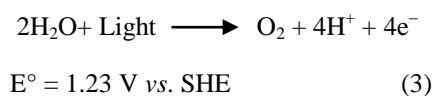
One major issue is the need to develop highly efficient photoactive materials capable of harvesting and converting solar energy into stored chemical energy, *i.e.* a clean non-fossil fuel like hydrogen. In the overall reaction of photosynthesis (Eqn. (1)), plants transform water and carbon dioxide in the presence of light into oxygen and carbohydrates. In effect then, H₂O is split into O₂ and H₂, where the hydrogen is not in the gaseous form but bound by carbon.



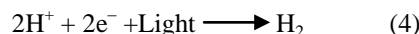
The photo-electrochemical (PEC) path to water splitting involves separating the oxidation and reduction processes into half-cell reactions. In equations (3) and (4) the half-cell reactions with their corresponding standard reduction potential E° with respect to the standard hydrogen electrode (SHE) are shown. Eqn. (5) shows the overall reaction and the corresponding ΔE°. The negative ΔE° indicates that water splitting is not a thermodynamically spontaneous process.

For the reaction to proceed, 1.23 V must be provided externally.

Oxidation:

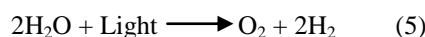


Reduction:



$$E^\circ = 0.00 \text{ V vs. SHE}$$

Overall:



$$\Delta E^\circ = -1.23 \text{ V}$$

Water splitting reaction is energy intensive and requires external energy to proceed. For this, three fundamental requirements should be by the semiconductor:

- The band gap of semiconductor should be more than 1.23eV.
- Appropriate band edges to carry out water oxidation and water reduction reaction.
- It should be chemically stable in the water.

This review focuses on photoelectrochemical approaches for splitting of water using inorganic semiconductors. It covers classical and more recent studies spanning approximately four decades.

II ELECTROLYSIS AND PHOTOELECTROLYSIS

In electrolysis of water, an external voltage of approximately 2.0 V is required which includes 1.23 V thermodynamic energy requirement and polarization losses but in photo assisted electrolysis of water this requirement is reduced but still the external voltage is required called as bias voltage as shown in Fig 1 (a). The semiconductor absorbs the light and produces electrons and holes. Electrons get conducted to cathode and holes oxidize water to produce oxygen and hydrogen ions as shown in Fig 1 (b).

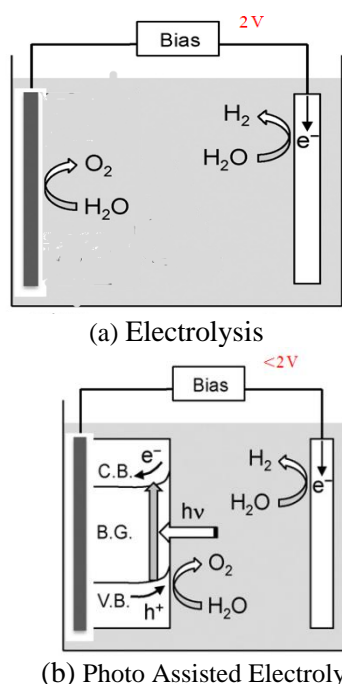


Fig 1: Bias Voltage Requirement for Electrolysis and Photo Assisted Electrolysis

Over 150 materials and derivatives are discovered either to catalyze the overall water splitting or cause water oxidation or reduction in presence of external redox agents. So far, no material capable of catalyzing overall water splitting having quantum efficiency larger than 10% has been found. Here 10% is the limit for commercial applications[1].

Many oxide semiconductors had been found to catalyze water oxidation or reduction reaction at low efficiencies and on irradiation of ultraviolet light like TiO_2 as shown in Fig 2.

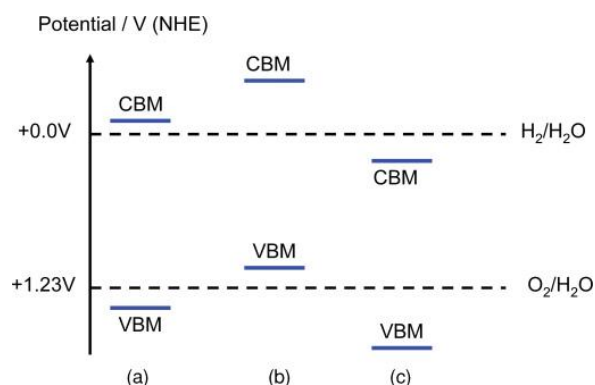


Fig 2: (a) Most desirable band edges position, (b) Only water reduction reaction possible, (c) Only water oxidation possible

However there are also many semiconductors like WO_3 which oxidizes water in visible region but unable to reduce hydrogen ions.

III LITERATURE SURVEY

Fujishima and Honda first discovered the water splitting using UV light and TiO_2 anode and platinum cathode [2]. In [3], authors showed the hydrogen produced by photoelectrolysis using platinized SrTiO_3 . In [4], authors explored the concept of photochemical diodes and showed the necessity of a bias potential for rutile photoanodes. Early studies on titanium dioxide semiconductors are given in Table 1. Titanium dioxide as a semiconductor has a band gap of 3.2 eV which corresponds to UV region. To narrow its band gap and bringing their responses in visible region doping with non metals were studied which is given in Table 2 and Table 3. In [5], authors studied the composite effects of CdSe with nitrogen TiO_2 and were able to narrow its band gap and brought the response in to the visible region. In [6], authors used Cu_2O layer protected by FTO layer for depositing the thin film of TiO_2 by atomic layer deposition. In [7], authors employed hydrothermal method and used TiO_2 nanoribbons morphology to narrow the band gap.

Table 1: Representative Early Study on TiO₂ Anodes

Title of the study	Comment	Reference
Electrochemical Photolysis of Water at a Semiconductor Electrode	First demonstration of the feasibility of water splitting	[2]
Photoassisted Electrolysis of Water by Irradiation of a Titanium Dioxide Electrode	The initial claim in Ref. 1 supported along with data on the wavelength response and the correlation of product yield and current	[3]
Improved Solar Energy Conversion Efficiencies for the Photocatalytic Production of Hydrogen via TiO ₂ Semiconductor Electrodes	Heat treatment of Ti metal found to influence performance	[8]
Novel Semiconducting Electrodes for the Photosensitized Electrolysis of Water	Appears to be the first study on doping TiO ₂ to extend its light response into the visible range of the electromagnetic spectrum.	[9]
An Effect of Heat Treatment on the Activity of Titanium Dioxide Film Electrodes for Photosensitized Oxidation of Water	Heat treatment in argon atmosphere found to improve performance of both anodic and pyrolytically prepared TiO ₂ films.	[10]

Table 2: Doping in Titanium Dioxide with Non Metals for Band Gap Narrowing

Title of the study	Comments	Reference
Visible-Light Photocatalysis in Nitrogen-Doped Titanium Oxides	Both films and powders considered. Substitutional doping with nitrogen shown to bring about band gap narrowing and also high photocatalytic activity with visible light. Experimental data supported with first-principles calculations.	[11]
Formation of TiO_2-xFx Compounds in Fluorine-Implanted TiO_2	Fluorine substituted for oxygen sites in the oxide by ion implantation.	[12]
Band Gap Narrowing of Titanium Dioxide by Sulfur Doping	Oxidative annealing of TiS_2 used. Ab initio calculations also reveal mixing of S 3p states with the valence bond to bring about band gap narrowing.	[13]
Efficient Photochemical Water Splitting by a Chemically Modified n- TiO_2	Combustion of Ti metal in a natural gas flame done to substitute carbon for some of the lattice oxygen sites. The photocatalysis performance data have been questioned	[14]
Visible Light-Induced Degradation of Methylene Blue on S-doped TiO_2	Oxidative annealing of TiS_2 used	[15]

Table 3: Recent Studies on TiO_2 Composite Electrode and Morphology

Title of the study	Comments	Reference
Synergistic effect of CdSe quantum dot sensitization and nitrogen doping of TiO_2 nanostructures for photoelectrochemical solar hydrogen generation	Study shows the sensitization of TiO_2	[5]
Highly active oxide photocathode for photoelectrochemical water reduction	Cu_2O atomic layer deposition on FTO substrate	[6]
Synthesis of TiO_2 nanoribbons and its application in photoelectrochemical water splitting for hydrogen production	bring about band gap narrowing and also high photocatalytic activity with visible light.	[7]

IV CONCLUSION

Titanium dioxide is a very stable semiconductor in aqueous conditions and economical but due to its large band gap it does not offers commercial application. But in last few years doping metals and non-metals and using composite electrodes with other semiconductors such as CdS, CdSe and Cu₂O, it is possible to narrow its band gap and solar light can be used to produce hydrogen. Overall efficiency of such anodes currently is not enough for commercial purposes but further research is going on to develop such anodes. With increase in prices of petroleum and coal it is going to be a viable alternative to produce hydrogen from solar light which is also environment friendly. The use of irradiated oxide semiconductor-liquid interfaces for hydrogen generation is now a mature field of research. Indeed, impressive results have been obtained at the laboratory scale over the past three decades and a range of new oxides are being continually discovered. On the other hand, much needs to be done to improve the H₂ generation efficiencies. The photoelectrolysis process must be engineered and scaled up for routine practical use. In this regard, oxide semiconductors appear to be particularly promising, especially from an environmental and process economics perspective. While interesting chemistry, physics, and materials science discoveries will continue to push this field forward, two types of R&D will be crucial: the use of composite semiconductors for electrodes development and innovations in reactor/process engineering once efficiencies at the laboratory scale have been optimized at a routinely attainable ~10% benchmark. Only then will the long sought after goal of efficiently making H₂ from sunlight and water using this approach be realized.

References

Journal Papers:

- [1] J. Nowotny, C.C. Sorrell, T. Bak, L.R., "Sheppard, Solar-hydrogen: Unresolved problems in solid-state science", *Solar Energy*, 78(5), 593-602.
- [2] A. Fujishima, K. Honda, "Electrochemical photolysis of water at a semiconductor electrode", *Nature*, 238 (5358), 1972, 37-38
- [3] M.S. Wrighton, P.T. Wolczanski, A.B. Ellis, "Photoelectrolysis of water by irradiation of platinized n type semiconducting metal oxides", *Journal of solid state chemistry*, 22, 1977, 17-29.
- [4] A.J. Nozik, R. Memming, "Physical chemistry of semiconductor-liquid interfaces", *Journal of physical chemistry*, 100(31), 1996, 13061-13078.
- [5] J. Hensel, G. Wang, Y. Li, J.Z. Zhang, "Synergistic Effect of CdSe Quantum Dot Sensitization and Nitrogen Doping of TiO₂ Nanostructures for Photoelectrochemical Solar Hydrogen Generation", *Nano letters*, 10, 2010, 478-483.
- [6] A. Paracchino, V. Laporte, K. Sivula, M. Gratzel, E. Thimsen, "Highly active oxide photocathode for photoelectrochemical water reduction", *Nature materials*, 10(6), 2011, 456-461
- [7] P.K. Dubey, R.S. Tiwari, O.N. Srivastava, A.S.K. Sinha, "Synthesis of TiO₂ nanoribbons and its application in photoelectrochemical water splitting for hydrogen production", *International Journal of Nanoscience*, 10, 2011, 723-726.
- [8] J. F. Houlihan, D. P. Madacs, E. J. Walsh, "Improved Solar Energy Conversion Efficiencies for the Photocatalytic Production of Hydrogen via TiO₂ Semiconductor Electrodes", *Material Research Bulletin*, 11 (9), 1976, 1191-1197.
- [9] J. Augustynski, J. Hinden, C. Stalder, "Novel Semiconducting Electrodes for the Photosensitized Electrolysis of Water", *Journal of Electrochemical Society*, 124 (7), 1977, 1063-1064.
- [10] Tamura H, Yoneyama H, Iwakawa C, Murai T, "An Effect of Heat Treatment on the Activity of Titanium Dioxide Film Electrodes for Photosensitized Oxidation of Water", *Bulletin of Chemical Society, Japan*, 50, 1977, 753.
- [11] R. Asahi, T. Morikawa, T. Ohwaki, K. Aoki, Y. Taga, "Visible-Light Photocatalysis in Nitrogen-Doped Titanium Oxides", *Science* 293, 2001, 269-271.
- [12] Yamaki T, Sumita T, Yamamoto S, "Formation of TiO_{2-x}F_x Compounds in Fluorine-Implanted TiO₂, *Material Science Letters* 21 (1), 2002, 33-35.
- [13] Umabayashi T, Yamaki T, Itoh H, Asai K, "Band Gap Narrowing of Titanium Dioxide by Sulfur Doping", *Applied Physics Letters*, 81: 454, 2002.
- [14] Khan SUM, Al-Shahry M, Ingler Jr WB, "Band Gap Narrowing of Titanium Dioxide by Sulfur Doping", *Science* 297, 2002, 2243.
- [15] Umabayashi T, Yamaki T, Tanaka S, Arai K, "Visible Light-Induced Degradation of Methylene Blue on S-doped TiO₂", *Chemistry Letters*, 32, 2003, 330.

Comparative Study of Different Algorithms for the Design of Adaptive Filter for Noise Cancellation

Shelly Garg^{*}, Ranjit Kaur^{**}

^{*}(Department of Electronics and Communication Engineering, Punjabi University, Patiala, India
Email: shellygarg96@gmail.com)

^{**} (Department of Electronics and Communication Engineering, Punjabi University, Patiala, India
Email:ranjit24_ucoe@pbi.ac.in)

ABSTRACT

The main goal of this paper is to study and to compare the performance of different adaptive filter algorithms for noise cancellation. Adaptive noise cancellation method is used for estimating a speech signal which is corrupted by an additive noise. The reference input containing noise is adaptively filtered and subtracted from the primary input signal to obtain the de-noised signal. The desired signal which is corrupted by an additive noise can be recovered by an adaptive noise canceller using Least Mean Square (LMS) algorithm, Data Sign algorithm, Leaky LMS algorithm and constrained LMS algorithm. A performance comparison of these algorithms based on Signal to Noise Ratio(SNR) is carried out using MATLAB.

Keywords-Adaptive Filter, Adaptive algorithms, MATLAB, Noise cancellation System, SNR

I INTRODUCTION

Noise is disturbance unwanted signal during communication. Noise can occur because of many factors like interference, delay, and overlapping. Noise problems in the environment are obtained due to the enormous growth of technology that has led to noisy engines, heavy machinery and other noise sources. Noise cancellation system employed for variety of practical applications such as the cancelling of various forms of periodic interference in electrocardiography, the cancelling of periodic interference in speech signals. Adaptive filtering has been extensively used in many practical applications. Important results have been obtained, for instance, in noise and interference cancelling for biomedical applications [1]. In the process of digital signal processing for noise or time varying signals, Finite Impulse Response (FIR) and Infinite Impulse Response (IIR) fixed coefficient filters cannot achieve optimal filtering. So, we must design adaptive filters, to provide the changes of signal and noise signal. Adaptive filter technology shows better performance as compared to conventional methods.

Section 2 gives an overview of adaptive filters. The brief description of noise cancellation system is made in section 2. The basic idea of an adaptive noise cancellation algorithm is to pass the corrupted signal through a filter that tends to suppress the noise signal while leaving the signal unchanged. This is an adaptive process, which means it does not require a priori knowledge of signal or noise characteristics.

Adaptive Noise Cancellation (ANC) completely attenuates the low frequency noise for which passive methods are ineffective. Section 4 introduces about adaptive algorithms such as Least Mean Square (LMS), Data Sign LMS, Leaky LMS, and Constrained LMS. Section 5 shows the results, observations and comparison of these algorithms on the basis of SNR. Section 6 concludes the main research work.

II ADAPTIVE FILTER

It is a filter that self-adjusts its transfer function according to the best algorithm operated by an error signal. Because of the complicated of these algorithms, most adaptive filters are digital filters. Adaptive filters are required for some applications because some parameters of the desired processing action are not known in progress [2] [3]. The adaptive filter uses feedback in the form of an error signal to filter its transfer function to associate the changing parameters. The adaptive process involves the use of a cost function which is a criterion for foremost performance of the filter, to deliver an algorithm, which determines how to alter filter transfer function to minimize the cost on the next iteration. Fig.1 shows the block diagram of adaptive filter [4].

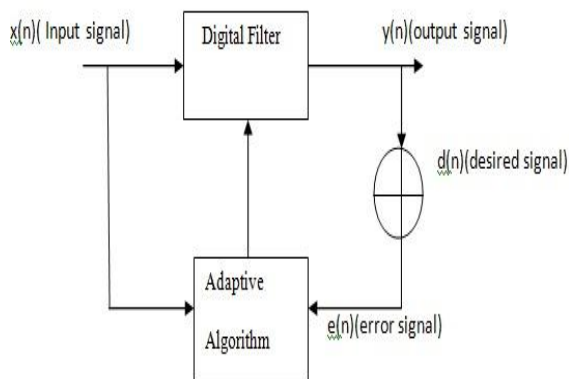


Fig 1: Block diagram of adaptive filter

III NOISE CANCELLATION SYSTEM

The general configuration of Noise Cancellation System [5] is shown in Fig.2. It has two inputs, the corrupted signal $d(n)$, which represents the desired signal $s(n)$ corrupted by an undesired noise $x_I(n)$, and the reference signal $x(n)$, which is the unwanted noise to be filtered out of the system. The goal of Noise Cancellation system is to reduce the noise signal, and to obtain the uncorrupted de-noised signal. In order to achieve this, a reference of the noise signal is required which is called as reference signal $x(n)$. However, the reference signal is usually not the same signal as the noise portion of the primary amplitude, phase or time. So, the reference signal cannot be simply subtract from the primary input signal to obtain the desired portion at the output. In general, noise that affects the speech signal can be modeled as White noise or Colored noise.

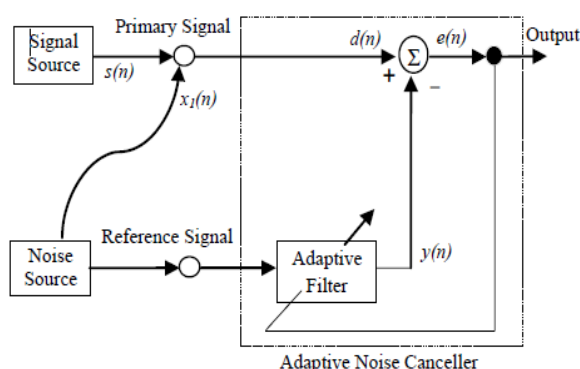


Fig 2: Adaptive noise cancellation system

Where $s(n)$ -source signal, $d(n)$ corrupted signal, $x_I(n)$ -noise signal, $x(n)$ -noise reference input, $y(n)$ -output of adaptive filter, $e(n)$ -system output signal.

Adaptive Noise Cancellation system utilize two signals, One signal is used to measure the speech with noise signal while the other signal is used to measure the noise signal alone. This technique adaptively adjusts a set of filter coefficients so as to remove the noise from the corrupted signal. This technique requires that the noise component in the corrupted signal and the noise in the reference signal have high coherence. Unfortunately this is a limiting factor, as the microphones need to be space apart in order to prevent the speech being included in the noise reference and thus it being removed. In summary, to realize an adaptive noise cancellation system we use two inputs and an adaptive filter. One input is the signal corrupted by noise which can be expressed as:

$$d(n) = s(n) + x_I(n) \quad (1)$$

The other input contains noise related in some way to that in the main input but does not contain anything related to the signal and it is known as noise reference input signal which can expressed as $x(n)$. The noise reference input pass through an adaptive filter and output $y(n)$ is produced as close a replica as possible of $x_I(n)$. The filter readjusts its filter coefficients itself continuously to minimize the error between $x_I(n)$ and $y(n)$ during this process. Then the output $y(n)$ is subtracted from the corrupted signal to produce the system output. It is represented as:

$$e(n) = s(n) + x_I(n) - y(n) \quad (2)$$

This is the de-noised signal.

IV ALGORITHMS OF ADAPTIVE FILTERS

The LMS adaptive filter family is very attractive for implementation of low-cost real-time systems due to its low computational intricacy and robustness [6] [7]. One of the most popular adaptive algorithms available in the literature is the stochastic gradient algorithm also called LMS [2] [3].

4.1 LMS Algorithm

This is extensively used for different applications such as channel equalization, echo cancellation and noise cancellation. The equation below is LMS algorithm for updating the tap weights of the adaptive filter for each iteration.

$$w(n+1) = w(n) + \mu e(n)x(n) \quad (3)$$

Where $x(n)$ is the input vector of time delayed input values and $w(n)$ is the weight vector at the time n . μ is the step size parameter. This algorithm is used due to its computational simplicity. It requires $2N+1$ multiplications and additions but it has a fixed step size for each iteration.

4.2 Data Sign LMS algorithm

In a high speed communication the time is critical, thus faster adaptation processes is needed

$$\text{sgn}(a) = \begin{cases} 1 & a > 0 \\ 0 & a = 0 \\ -1 & a < 0 \end{cases} \quad (4)$$

For data Sign algorithm [7] weight update coefficients equation is:

$$w(n+1) = w(n) + 2\mu e(n) \text{sign}(x(n)) \quad (5)$$

By introducing the signum function and setting μ a value of power of two, the hardware implementation is highly simplified. It improves the convergence behavior, requires less computational complexity and also provides good result but throughput is slower than LMS Algorithm.

4.3 Leaky LMS Algorithm

It introduces a leakage coefficient into LMS algorithm so it becomes as:

$$w(n+1) = (1 - 2\mu\gamma)w(n) + 2\mu e(n)x(n) \quad (6)$$

Where $0 < \gamma \ll 1$. The effect of introducing the leakage coefficient γ is to force any undamped modes to become zero and to force the filter coefficients to zero if either $e(n)$ or $x(n)$ is zero.

4.4 Linearly constrained LMS Algorithm

In LMS algorithm, no constrain was imposed on the solution of minimizing the MSE. However, in some applications there might be some mandatory constraints that must be taken into consideration in solving optimization problems. The problem of minimizing the average output power of a filter while the frequency response must remain constant at specific frequencies. In this we discuss the filtering problem of minimizing the MSE subject to a general constraint. This algorithm has following two steps:

Step 1: $w'(n) = w(n) + 2\mu e(n)x(n) \quad (7)$

Step 2: $w(n+1) = w'(n) + \eta(n) \quad (8)$

using the Lagrange multiplier method that gives where

$$\eta(n) = \frac{a - c^T w'(n)}{c^T c} c \quad (9)$$

To obtain final form:

$$w(n+1) = w'(n) + \frac{a - c^T w'(n)}{c^T c} c \quad (10)$$

Where c is constant vector and a is constraint constant.

V RESULTS AND OBSERVATIONS

SNR is defined as the power of the desired signal divided by the noise power. It is measured in

Decibel(dB).It is a measure used in science and engineering that compares the level of a desired signal to the level of background noise.

$$SNR_{dB} = 10 \log_{10} \left(\frac{P_{signal}}{P_{noise}} \right) \quad (11)$$

.The simulation results show that LMS, Data Sign LMS, Leaky LMS, Linearly Constrained LMS algorithms are used to cancel the noise and provides good results. Convergence of the adaptive for the choices of step size parameter μ which is constant is very sensitive. The order of the filter was set to $M=40$. Original input signal having sampling frequency 500Hz is corrupted by adding white Gaussian noise. No. of Samples is 4000. No of iterations are same as no. of samples. The value of parameter μ varies for all algorithms for good result.

Frequency response of de-noised signal should be same as the original signal. This can be achieved by using different types of algorithms. Fig. 3 shows the original signal, corrupted signal and reference input signal. Fig. 4 shows the frequency response of original signal and corrupted signal. The parameter μ is set to 0.001. Fig.5 shows the frequency response of de-noised signal by using LMS algorithm. Fig.6 shows the frequency response of de-noised signal by using Data Sign LMS. Fig.7 shows the frequency response of de-noised signal by using leaky LMS. Fig.8 shows the frequency response of de-noised signal by using linearly Constrained LMS. Table 1 show that the results of linearly Constrained LMS are better than LMS, Sign LMS and Leaky LMS.

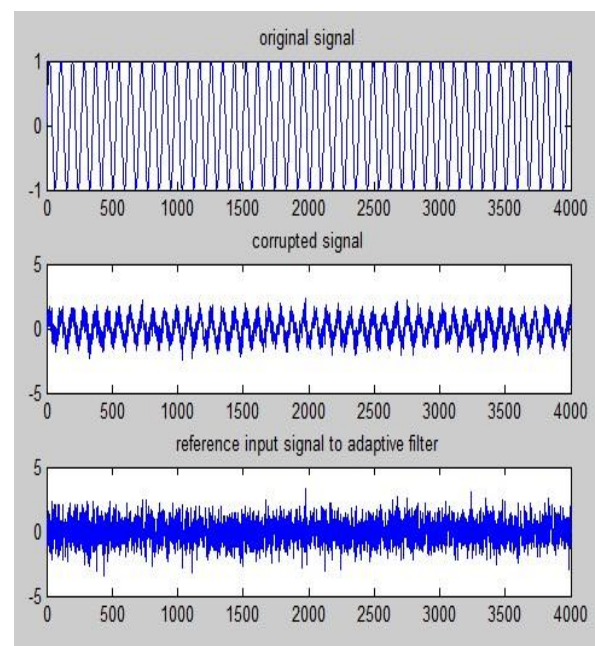


Fig 3: Original signal, corrupted signal and reference input signal

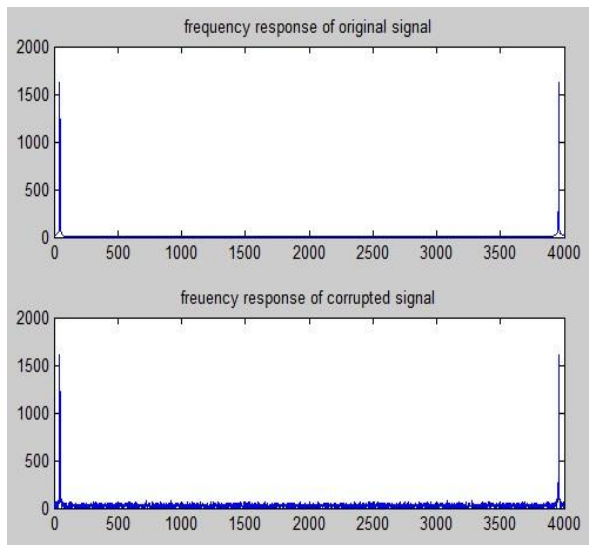


Fig 4: Frequency response of original signal and corrupted signal.

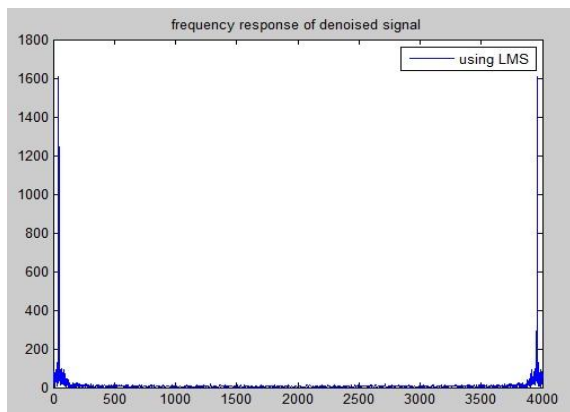


Fig 5: Frequency response of de-noised signal by using LMS algorithm

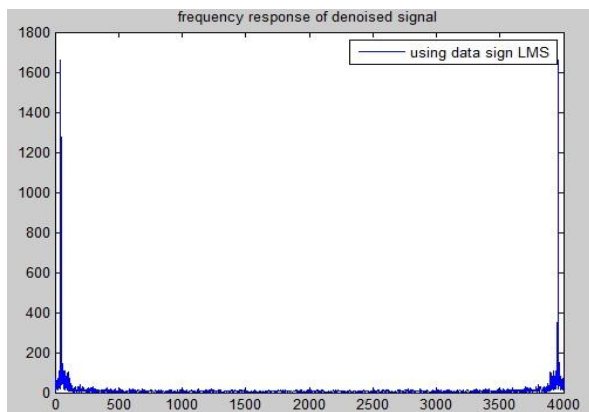


Fig 6: Frequency response of de-noised signal by using data Sign LMS.

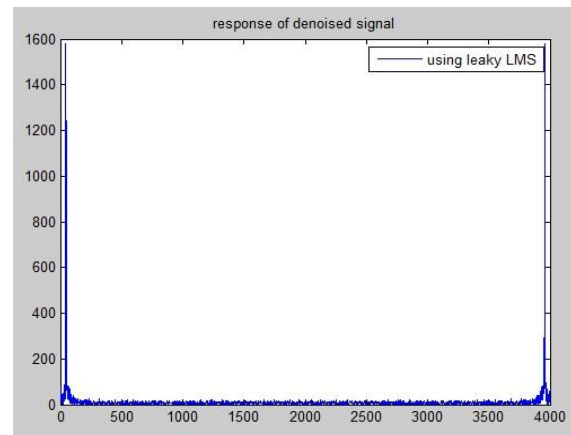


Fig 7: Frequency response of de-noised signal by using leaky LMS

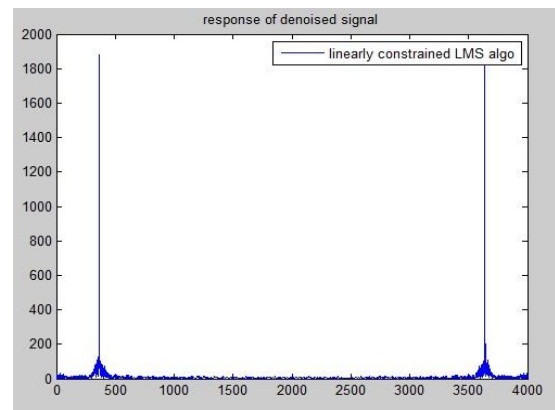


Fig 8: Frequency response of de-noised signal by using linearly constrained LMS

Table 1: Performance Comparison

Algorithms	SNR before(dB)	SNR after (dB)
LMS	-1.8887	10.34
Data-Sign LMS	-1.9676	10.478
Leaky LMS	-2.1013	11.5701
Linearly Constrained LMS	-1.9631	11.7829

VI CONCLUSION

From the above discussion, it has been concluded that four different types of adaptive algorithms are used for noise cancellation and for improving SNR after adaptive filtering. Linearly Constrained LMS algorithm provides high SNR as compared to LMS, Data Sign LMS, and Leaky LMS algorithms. The future work will be directed to determine SNR using Error Data Normalized steady state (EDNSS) algorithm.

REFERENCES

- [1] N.V.Thakor, and Y.S. Zhu, "Applications of adaptive filtering to ECG analysis: noise cancellation and arrhythmia detection," *IEEE Trans. on Biomedical Engineering*, 38(8), 1991, 785-794.
- [2] X.N. Fernando,S.Krishnan,and H. Sun., "Non-stationary interference cancellation in infrared wireless receivers," *Proc. IEEE Canadian conference on Electrical and Computer Engineering*, 2003, 1-5.
- [3] A.Th.Schwarzbach, and J.Timoney, "VLSI," *Irish signal and system Conference*, 2000, 368-375.
- [4] H.Kaur, Dr.R.Malhotra, and A. Patki, "Performance Analysis of Gradient Adaptive LMS Algorithm," *International Journal of Scientific and research publications*, 2(1), 2012, 1-4.
- [5] G. Singh, K .Savita,S.Yadav,andV.Purwar, "Design of Adaptive Noise Canceller using LMS Algorithm," *International Journal of Advanced Technology & Engineering Research (IJATER)*, 3(3), 2013.
- [6] D. G. Manolakis, V. K. Ingle, and S. M. Kogon, "Statistical and adaptive signal processing, Spectral Estimation, Signal Modeling, Adaptive Filtering and Array Processing", *Artech House Publishers*, 2000.
- [7] T.Lalith Kumar, and Dr.K.Soundara Rajan "Noise Suppression in speech signals using Adaptive algorithms", *International Journal of Engineering Research and Applications (IJERA)*, 2(1), 718-721, 2012.

Bandwidth Enhancement Technique For Microstrip Patch Antenna For WLAN Application

Amit Joon*, Anjali Grover**, Pranav Sharma ***, Prateek Rao****, Vikas*****

* (Department of Electronics and Communication, Amity University, Haryana
Email: amitsinghjoon@gmail.com)

** (Department of Electronics and Communication, Amity University, Haryana
Email: anjali.grover@outlook.com)

*** (Department of Electronics and Communication, Amity University, Haryana
Email: pranavsharma300@gmail.com)

**** (Department of Electronics and Communication, Amity University, Haryana
Email: pranav792rao@gmail.com)

***** (Department of Electronics and Communication, Amity University, Haryana
Email: vikas_kharanger@hotmail.com)

ABSTRACT

This communication presents a method to enhance the bandwidth of microstrip antenna by cutting a slot in the patch. Firstly, an antenna using inset microstrip line feed is designed for 5.2 GHz WLAN application. The bandwidth of antenna is found to be 170 MHz; which increases to 236 MHz when a rectangular slot is cut from the patch. The directivity of both the antennas resonating at 5.2 GHz is found to be 5.89 dB. CST studio is used as the software tool. Duroid substrate having a dimension of 28 mm × 36 mm × 1.604 mm is used as the base of the antenna, giving the volume of the antenna to be 1.616 cm³. Thus, this volume makes the antenna suitable for WLAN application.

Keywords: Directivity, Duroid, Microstrip, Resistance, Wireless Local Area Network (WLAN).

I. INTRODUCTION

Microstrip is probably the most successful and revolutionary antenna technology. Its success stems from very-well-known advantageous and distinctive properties, such as a low profile, light weight, planar structure (but also conformal to non-planar configurations), mechanical robustness, easy (simple and low-cost) fabrication, easy integration of passive and active components, easy incorporation in arrays, and notable versatility in terms of electromagnetic characteristics (resonant frequency, input impedance, radiation pattern, gain, polarization).

Primary barriers to implement patch antennas in modern broadband communication system applications are their narrow bandwidth. The microstrip antennas are often realized with bandwidth of the order of 1% to 5% [1] [2]. Bandwidth enhancement technique is one of the areas of research in the field of microstrip antennas. Basically the bandwidth is defined more concisely as a percentage $(f/f_0) \times 100\%$, where f and f_0 respectively represent

the width of the range of acceptable frequencies and the resonant frequency of the antenna. The parameters such as radiation efficiency, return loss, and voltage standing wave ratio (VSWR) are often used to define the bandwidth of a microstrip antenna [3]. This paper experimentally investigates an alternative approach in enhancing the bandwidth of microstrip antenna for the Wireless Local Area Network (WLAN) application operating at a frequency of 5.2 GHz. The result of this paper will show that enhancement of the original bandwidth can be achieved by using slot with proper position selection. The bandwidth, gain and radiation pattern are evaluated using CST software.

II. LITERATURE REVIEW

Microstrip patch antenna consists of a radiating patch which is generally made of conducting material such as gold or copper and can take any possible shape [9]. The radiating patch and the feed lines are usually photo etched on the dielectric substrate which has a ground plate as

shown in Fig. 1. In order to simplify analysis and performance prediction, the patch is generally square, rectangular, circular, triangular, and elliptical in shape.

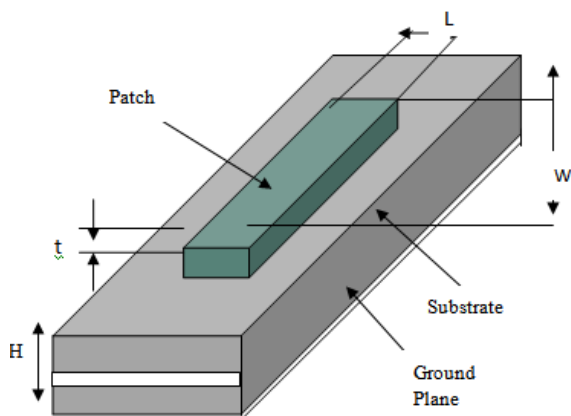


Figure 1: Structure of Microstrip patch antenna

For a rectangular patch, the length L of the patch is usually $0.333\lambda_0 < L < 0.5\lambda_0$, where λ_0 is the free space wavelength. The patch is selected to be very thin such that the patch thickness $t \ll \lambda_0$. The height h of the dielectric constant of the substrate (ϵ_r) is typically in the range $2.2 \leq \epsilon_r \leq 12$. The microstrip patch antenna radiates primarily because of the fringing fields between the patch edge and the ground plane. For good antenna performance, the choice of substrate used is an important factor. There are numerous substrates that can be used for the design of microstrip antennas within the dielectric constants range of $2.2 \leq \epsilon_r \leq 12$. The low dielectric constant ϵ_r is about 2.2 to 3, the medium around 6.15 and the high approximately above 10.5 [4] [5]. A thick dielectric substrate having a low dielectric constant is desirable since this provides better efficiency, larger bandwidth and better radiation. However, such a configuration leads to a larger antenna size. In order to design a compact microstrip patch antenna, substrate with higher dielectric constants must be used which are less efficient and result in narrower bandwidth. Hence, a trade-off must be realized between the antenna dimensions and antenna performance [6] [7] [8].

III. PROPOSED METHODOLOGY

Firstly, an antenna using inset microstrip line feed will be designed for 5.2 GHz WLAN application. The specifications of the antenna are calculated as per the requirement. The parameters then used are shown in Table 1. Further we cut a rectangular slot from the patch and analyse the return

loss graph to measure the bandwidth difference between antenna without slots and the one with slots. Directivity will also be studied on the CST studio. CST studio will be used as the software tool.

Table 1: Microstrip antenna parameters used

Name	Value
Fi	4.5
Gpf (Gap between patch and feed)	1.49
L (Length of patch)	12
Lf (Length of feed)	11
Mt (Thickness of copper layer on FR4 substrate)	0.1
W (Width of patch)	17.7
Wf (Width of feed)	3
H (Thickness of substrate)	1.6

IV. ANTENNA GEOMETRY

4.1 Without Slot Geometry

Fig 2 shows a basic microstrip antenna. Ground plane is actually beneath the patch but it is shown above the substrate, as the figure depicts a 3D antenna.

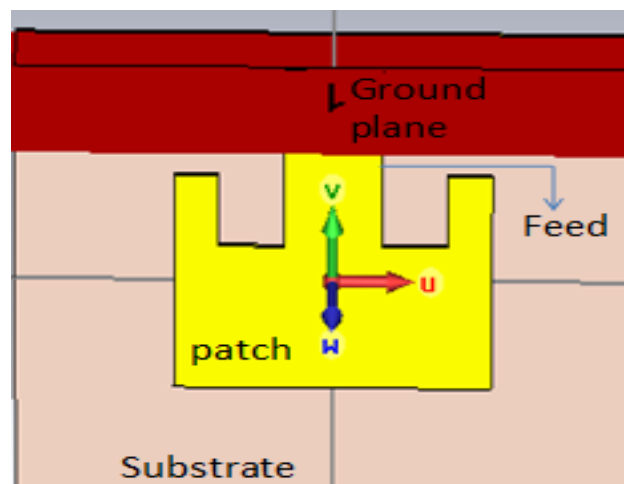


Figure 2: Microstrip antenna without slot

4.2 Slot Geometry

In Fig. 3, a rectangular microstrip antenna is shown after the introduction of slot. The dimensions of the slot are

$$\begin{aligned}
 U_{min} &= -1 \\
 U_{max} &= +1 \\
 V_{min} &= -4 \\
 V_{max} &= +4
 \end{aligned}$$

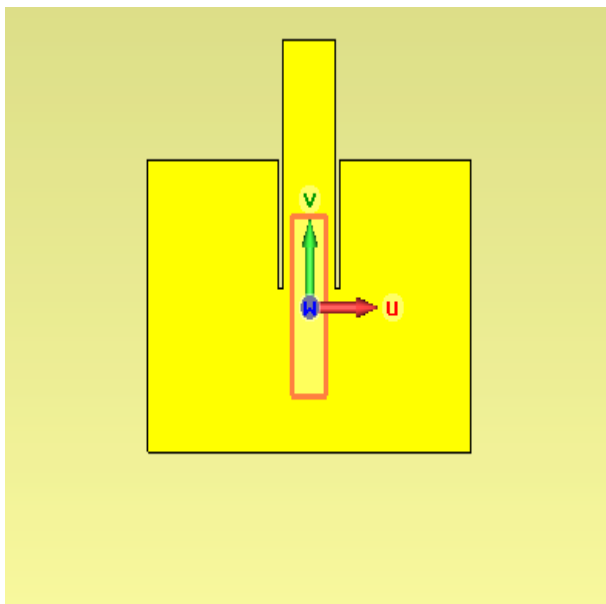


Figure 3: Microstrip antenna with slot

V. RESULT AND DISCUSSION

a. Return Loss

The return loss is a way of expressing mismatch. It is a logarithmic ratio measured in dB that compares the power reflected by the antenna to the power that is fed into the antenna from the transmission line. The relationship between VSWR and return loss is as follows [7]. In Fig 4, we see the return loss graph, where the dip is greater in case of antenna with slot.

$$\text{Return loss in dB} = 20 \log_{10} \frac{(VSWR)}{(VSWR - 1)} \quad (1)$$

The bandwidth difference increases from $d=0.1684$ to $d=0.2303$ on introducing the slots in microstrip patch antenna.

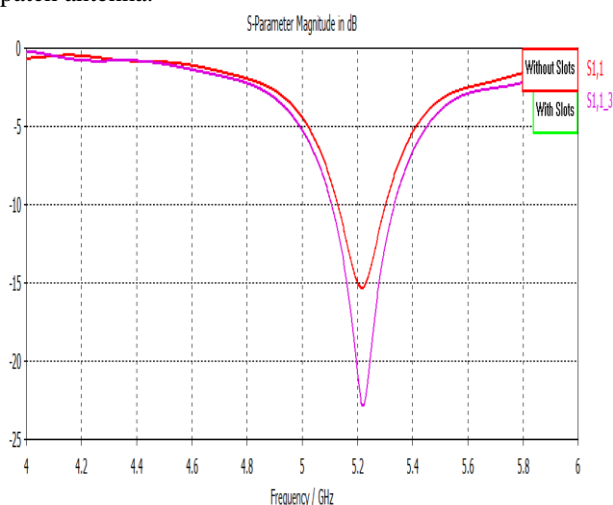


Figure 4: Simulated Return Loss Graph with and without slots.

5.2 Directivity

Directivity may be defined as the ratio of maximum radiation intensity of the test antenna to its average radiation intensity. Alternatively, Directivity is the ratio of maximum radiation intensity of the subject antenna to the radiation intensity of an isotropic antenna radiating the same total power. The directivity is fairly insensitive to the substrate thickness [8-9]. It is higher for lower permittivity, because the patch is larger.

The directivity plots with and without slots are shown in Fig. 5 and Fig. 6 respectively.

5.2.1 Antenna without slots

As in Fig. 5, at frequency 5.2 GHz, Main lobe magnitude comes out to be 6.9dBi. Main lobe direction and angular width are 1.0 degree and 97.4 degree respectively. The side lobe level is found to be -13.4dB.

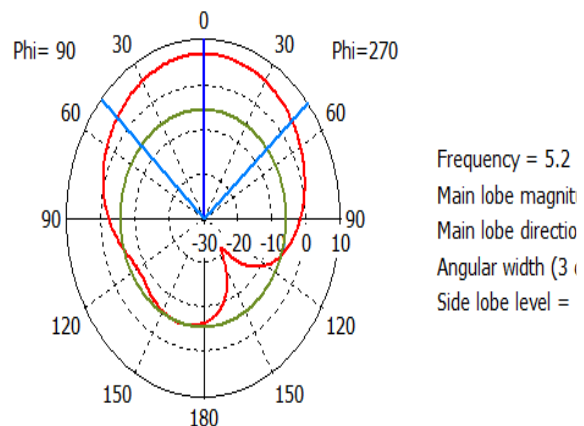


Figure 5: Plot of Theta/Degree vs. dBi

5.2.2 Antenna with slots

Now, in Fig. 6 we see that on the introduction of slots, at the same frequency, that is, 5.2 GHz, main lobe magnitude becomes 6.9dBi, main lobe direction 1.0 degree, angular width 97.1 degree and side lobe level 13.4dB.

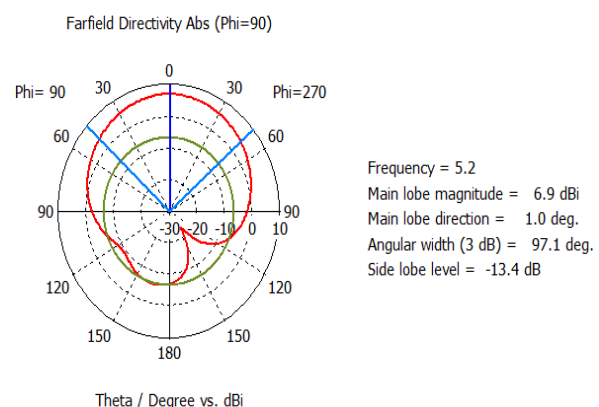


Figure 6: Plot of Theta/Degree vs. dBi

VI. CONCLUSION

The microstrip patch antenna has restricted and narrow bandwidth. We used slot cutting technique to increase the bandwidth. The results obtained clearly show that the bandwidth of the microstrip antenna increases on the introduction of slots and it can be used for WLAN applications. The advantage of this technique is that it does not increase the lateral size of the microstrip antenna. However, the height of microstrip antenna is increased.

REFERENCES

Journal Papers:

- [1] K.T Ahmed, M. B Hossain and M.J Hossain, Designing a high bandwidth patch Antenna comparison with the former patch Antenna *Canadian journal on multimedia and wireless network Vol.2*, No. 2 April,2011.
- [2] X.-S. Yang, B.-Z. Wang, S. H. Yeung, Q. Xue, and K. F. Man, Circularly Polarized Reconfigurable Crossed-Yagi Patch Antenna, *IEEE Antennas and Propagation Magazine*, vol. 53, pp. 65 - 80, 2011.
- [3] K. Deb, A. Pratap, S. Agrawal, and T. Meyarivan, A fast and elitist multiobjective genetic algorithm: NSGA-II, *IEEE Trans. on Evolutionary Computation*, vol. 6, pp. 182–197, April 2002.

Thesis:

- [4] K. P Ray, *Broadband, dual-frequency and compact microstrip Antennas*, Ph.D Thesis, Indian Institute of Technology, Bombay, India, 1999.
- [5] S.K Behera, *Novel Tuned Rectangular Patch Antenna as a load for phase power combining*, Ph.D Thesis, Jadavpur University, Kolkata, India.

Proceedings Papers:

- [6] D. M. Pozar, *Microstrip Antennas*, *Proc.of the IEEE*, vol. 80, pp. 79 – 91, January 1992.
- [7] H. Pues and A. V Capelle, *Accurate transmission-line model for the rectangular microstrip antenna*, *Proc. IEEE*, vol. 131, no.6, pp. 334-340, December 1984.

Books:

- [8] Y. Rahmat Samii and E. Michielssen, *Electromagnetic optimization by genetic algorithms*, J. Wiley & Sons, 1999.

- [9] J. R James and P. S Hall, *Handbook of microstrip Antennas*, Volume . Peter Peregrinus Ltd, London, 1989.

Tuning Techniques of PID controller: A Review

Avtar Singh*, Amrit Kaur**

*(Department of Electronics & Communication Engineering, Punjabi University, Patiala, Punjab-India
 Email: avtar2030@gmail.com)

** (Department of Electronics & Communication Engineering, Punjabi University, Patiala, Punjab-India
 Email: amrit_aks@yahoo.ca)

ABSTRACT

PID controller is widely used in industries and tuning of PID controller is an important parameter to obtain the optimal values. Different techniques are used for the tuning purpose of PID controller which can be categorized as conventional tuning techniques that are developed for PID tuning and metaheuristic optimization algorithms that are applied to the tuning of PID controller. The main aim of this paper is to provide an overview of tuning techniques of PID controller.

Keywords – conventional techniques, metaheuristic techniques, PID controller, Tuning.

I. INTRODUCTION

PID controller is widely used in industry to control the specific systems such as Automatic Voltage Regulator system and hydraulic system etc. PID controller has three parameters proportional k_p , integrative k_i and derivative k_d . These three parameters have their own importance in controlling purpose. The transfer function of PID is given as:

$$C(s) = K_p + \frac{K_i}{s} + k_d s = \frac{k_d}{k_p} K_p \left(1 + \frac{1}{T_i s} + T_d s \right)$$

Where k_p =proportional Gain, k_i =Integral Gain,

k_d =Derivative Gain, T_i =Reset Time = $\frac{k_p}{k_d}$,

T_d =Rate Time or derivative time = $\frac{k_d}{k_p}$.

The basic diagram of PID controller is shown in Fig.1,

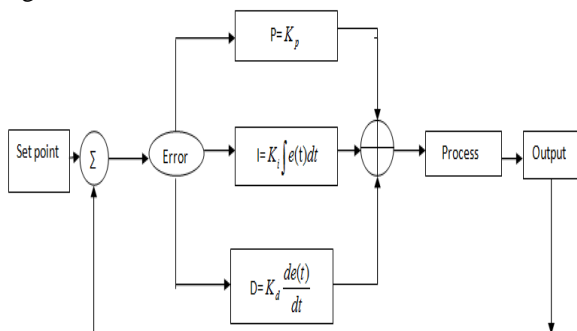


Figure 1: Block Diagram of PID Controller

where *Rise Time* is the time taken by a signal to change from a specified low level to a specified high level, *Settling Time* is the time required for the response curve to reach and stay within a range of specified percentage of the final value and *Maximum overshoot* is the maximum peak value of the response that is measured corresponding to the desired value. The effect of increasing the parameter of PID controller is shown in table 1.

Table 1: Effect of Parameters

Parameter	Rise Time	Settling Time	Overshoot	Steady State error
k_p	Decrease	Small change	Increase	Decrease
k_i	Decrease	Increase	Increase	Eliminate
k_d	Minor change	Decrease	decrease	No effect

Tuning techniques are classified as:

1.1 Conventional Techniques

Conventional techniques are based on the assumptions about the plant and the desired output. The assumptions are drawn analytically or graphically which are then used for the setting of controller parameter. These conventional techniques are very fast. But because of assumptions made, the required results are not obtained and so additional tuning is required. A few conventional techniques are discussed in this paper.

1.2 Metaheuristic Optimization Techniques

In computer science and mathematical optimization, a metaheuristic is a higher level procedure that is

designed to find and generate a sufficient good solution to optimization problems. These optimization techniques basically use the cost or objective function. The objective or cost function is a function of some variable of the optimization problem and so the main goal of the optimization technique is to minimize the cost or objective function by comparing it with their previous iteration result.

This paper is organized as: section 2 describes different types of conventional techniques, section 3 describes different types of metaheuristic optimization techniques and hence conclusion is drawn in section 4.

II. CONVENTIONAL TECHNIQUES

Some of the conventional techniques are discussed as follows:

2.1 Zeigler-Nichols Method

Zeigler-Nichols is a heuristic tuning rule used to obtain the optimal values of three parameters of PID controller and there exist two Zeigler-Nichols methods. In first method, if plant does not consists of integrator or dominant complex conjugate poles, then such a unit step response of curve may look like S-shaped curve as shown in fig.2. The S-shaped curve is characterized by two constants, delay L and time constant T. This method is used to tune PID controller for spindle motor system [1].

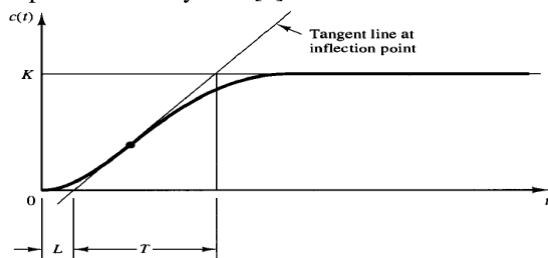


Figure 2: S-Shaped Response Curve

Table 2:Zeigler Nichols Tuning Rule First Method

Controller	k_p	k_i	k_d
P	$\frac{T}{L}$	∞	0
PI	$0.9 \frac{T}{L}$	$\frac{L}{0.3}$	0
PID	$1.2 \frac{T}{L}$	$2L$	$0.5L$

In second method, proportional controller is used only, K_p increases from 0 to a captious value K_{cr} at which the output first shows the sustained oscillations. Thus the captious gain K_{cr} and

corresponding period P_{cr} are experimentally determined and PID parameter setting is given in [1].

2.2 Cohen Coon Method

Cohen and Coon [2] design method for the tuning of PID controller parameters and decision is based on a FOLPD model. The main design requirement is the rejection of load disturbances. The controller parameter settings are given in [2]. Despite a better model, the results of the Cohen Coon method are not much better than the Ziegler Nichols method

III. METAHEURISTIC OPTIMIZATION TECHNIQUES

Some of the optimization algorithms are discussed as follows:

3.1 Particle Swarm Optimization

Particle swarm optimization (PSO) algorithm is one of the optimization techniques and is found to be robust in solving non-linear, non-differentiable problems.

The PSO is motivated from social behavior of bird flocking. It uses a number of particles which fly around in the search space to find best solution. By the meantime, they all look at the best particle (best solution) in their paths. In additional words, particles consider their own best solutions as well as the best solution has found so far that is birds follow the bird which is nearest to the food. Every particle in PSO should consider the current position, the current velocity, the distance to pbest, and the distance to gbest to modify its position. Mathematical equation of PSO algorithm is given as[3]:

$$v_i^{(t+1)} = w * v_i^t + c_1 * rand * (pbest_i - x_i^t) + c_2 * rand * (gbest - x_i^t) \quad (1)$$

$$x_i^{(t+1)} = x_i^t + v_i^{(t+1)} \quad (2)$$

$i=1,2,3 \dots n$

n =number of particles

t =pointer of iteration

w =inertia weight factor

$w = w_{mx} - ((w_{mx} - w_{mi}) / \text{maxIterations}) * \text{iterationCount}$;

c_1, c_2 =acceleration constant.

$rand$ =random number between 0 to 1;

x_i^t =current position of i^{th} particle.

v_i^t =velocity of particle i at iteration t .

$pbest_i = pbest_i$ of agent i at iteration t

The PSO starts randomly by placing the particles in problem space. In every iteration velocity of the particles calculated using equation (1) and then current position is updated using equation (2). The process of updating position of the particles continue until the desired results are not obtained. PSO algorithm has been implemented for tuning of PID for Automatic Voltage regulator system [4]. Author

gives the comparison of PSO-PID tuning with GA-PID tuning and it found that PSO-PID gives better result as compared to GA-PID.

3.2 Artificial Bee Colony Algorithm (ABC)

Artificial bee colony algorithm is an optimization technique in computer science and operation research and is based on the intelligent foraging behavior of honey bee swarm.

In Artificial Bee Colony (ABC) algorithm, colony consists of three categories of bees: employed bees, onlookers and scouts. First half of the colony consists of the employed bees and second half consists of onlookers. For every food source, there is only one employed bee. In other words, the number of employed bees is equal to the number of food sources around the hive that is the relationship between the employed bees and food sources is one to one. The employed bee whose food source has been deserted by the bees becomes a scout. A possible solution to the optimization problem is given by the position of a food source and the nectar amount of a food source corresponds to the quality or fitness of the associated solution. The number of employed bees or the onlooker bees is equal to the number of solutions in the population. ABC algorithm is an iterative algorithm starts by associating each employed bee with randomly generated food source. In each iteration, each employed bee discovers a food source in its neighborhood and evaluates its nectar amount or fitness using equation (3), and is given as [5]:

$$v_{nj} = x_{nj} + \psi_{nj} * (x_{nj} + x_{mj})$$

(3) Where v_{nj} = new food source;

x_{nj} = food source;

ψ_{nj} = random number between -1 to +1;

x_{mj} = randomly selected food source;

If fitness of new food source is better than the fitness of the old fitness value then employed bee moves to the new source otherwise it retain the old one. After all employed bees complete the search process, they share the information about their food sources with onlooker bees. An onlooker bee evaluate the nectar information taken from all the employed bees and choose a food source with a probability p_n that is proportional to the fitness of the food sources as given by following equation (4)

$$p_n = \frac{fit_n}{\sum_{n=1}^k fit_n} \quad (4)$$

Where fit_n is the fitness value of the solution n which is proportional to the nectar amount of the food source in the position n and k is the number of food sources which is equal to the number of employed bees. The employed bees become scout bees when a food source which is exhausted by the employed and onlooker bees is assigned as deserted. In that position, scout generates randomly a new solution by equation (5):

$$x_n^j = x_{min}^j + rand(0,1)(x_{max}^j - x_{min}^j) \quad (5)$$

j=1,2,3----D

ABC has been implemented for tuning of PID for speed control of DC motor [6]. Author compared the performance of DC motor with tuning of PID controller conventional tuning techniques and artificial bee colony algorithm and it is found artificial bee colony algorithm is best among the other tuning methods.

3.3 Genetic Algorithm

Genetic algorithm has been widely studied, experimented and applied in handling high dimensional and non-linear problems. Genetic algorithm is an optimization technique based on the mechanism of natural selection. GA starts with an initial population containing a number of chromosomes where each one represents a solution of the problem from which performance is evaluated by a fitness function.

Basically, GA consists of three main stages: selection, Crossover and Mutation. The application of these three basic operations allows creation of new individuals which may be better than their parents. This algorithm is repeated for many generations and finally stops when reaching individuals that represents the optimum solution to the problem. The flowchart of GA is shown in fig. 3 [7].

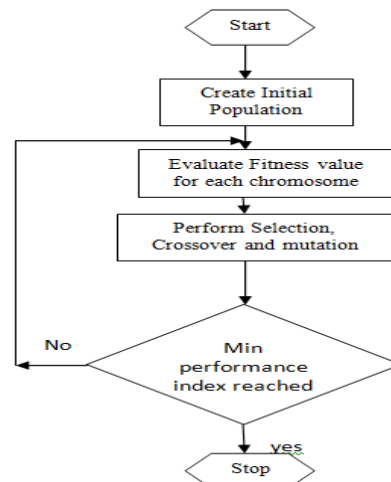


Figure 3: Flow Chart for Genetic Algorithm

Genetic algorithm has been implemented for tuning of PID controller for hybrid electric vehicle [8]. Author compared the performance of hybrid electric vehicle with tuning of PID controller conventional tuning technique such as Zeigler-Nichols method and Genetic Algorithm and it is found that genetic algorithm is best among other technique.

3.4 Firefly Algorithm

Firefly algorithm is an optimization technique inspired by the flashing behavior of fireflies.

Firefly's flash is act as a signal to attract other fireflies.

According to the law of inverse square, light intensity decreases as the distance r increases as by a relation as $I \propto \frac{1}{r^2}$.

Some ideology for Firefly algorithm is given as [9]

- a. All fireflies are unisex so that one firefly will attracted to other fireflies regardless of their sex.
- b. Attractiveness is proportional to their brightness; thus for any two flashing fireflies, the less bright one will move toward the brighter one. The attractiveness is proportional to the brightness and they both decrease as their distance increases. If there is no brighter one than a particular firefly, it will move randomly.
- c. The brightness of a firefly is affected or determined by objective function.

In this algorithm, each firefly has a location X in d-dimension space and light intensity I(x) or attractiveness $\beta(x)$, which is proportional to the objective function f(x). The attractiveness β is given as in equation (6) [9];

$$\beta = \beta_0 \exp(-\gamma * r^2) \quad (6)$$

Where r is the distance between the two fireflies i and j at x_i and x_j respectively, β_0 is attractiveness at r=0 and is the light absorption coefficient in the environment. The initial solution is generated as:

$$x_j = rand \times (ub - lb) + lb \quad (7)$$

Where ub and lb is upper and lower limits. Each firefly i can move toward another more attractive firefly j by

$$x_i^{t+1} = x_i^t + \beta \exp(-\gamma r_{ij}^2) + \alpha_i (rand - \frac{1}{2}) \quad (8)$$

Where α is a significance factor of the randomize parameter and rand is random number between 0

to 1. the distance between two fireflies i and j at x_i and x_j respectively is given as:

$$r_{i,j} = \|x_i - x_j\| = \sqrt{\sum_{k=1}^d (x_{i,k} - x_{j,k})^2} \quad (9)$$

Where $x_{i,k}$ is the k^{th} component of the spatial coordinate x_i of the i^{th} firefly.

Firefly algorithm has been implemented for the tuning of PID controller [10]. Author compared the performance of PID controller conventional tuning technique such as Zeigler-Nichols method with Firefly algorithm and it is found that Firefly algorithm is best among other technique.

3.5 Fuzzy Logic

Fuzzy logic control is one of the interfaces between control engineering and artificial intelligence. The Fuzzy logic controller (FLC) adds to the conventional PID controller to adjust the parameters of the PID controller on-line according to the change of the signals error and change of the error. The design specifications of the FLC vary with the plant being used and the PID controller parameter ranges in combination with which it is to be used. The basic building block of the controller remains similar. Fig.4 shows the commonly used Fuzzy Logic Control [11].

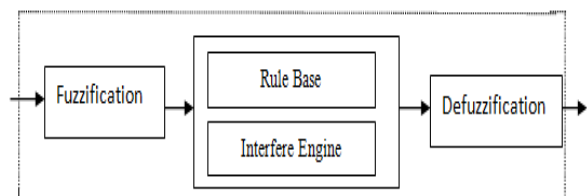


Figure 4: Fuzzy Logic Control

As shown in Fig. 5, the error and derivative of the error are inputs to the fuzzy interface. The model most commonly employed in the fuzzy interface is the Mamdani model. The operation of the Mamdani rule base can be broken down into four parts,

1. Mapping each of the crisp set into fuzzy variable (fuzzification).
2. Determining the output of each rule given its fuzzy antecedents;
3. Determining the whole output(s) of all fuzzy rules;
4. Mapping the fuzzy output(s) to crisp output(s) (defuzzification).

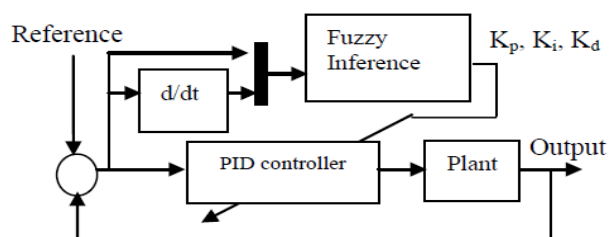


Figure 5: Block Diagram of FLC Based Controller

Fuzzy logic has been implemented for the tuning of PID controller [12]. Author compared the performance of PID controller tuning conventional techniques and such as Zeigler-Nichols method with Fuzzy logic and it is found that fuzzy logic is best among them.

IV. CONCLUSION

A number of techniques for the tuning of PID controller are reviewed in this paper. A brief discussion of the techniques followed by its implementation by various authors is indicated for tuning and self tuning of PID controller. From the above discussion, it is found that metaheuristic optimization techniques gives correct and object oriented results as compared to conventional techniques.

REFERENCES

[1] K. Ogata, PID controls and Two-Degree Of freedom control system in *Modern Control Engineering*, (India: Pearson Education,2002) 681-751

[2] G. H. Cohen, and G. A. Coon, "Theoretical considerations of retarded control," *Transactions of ASME*, 75(1), 1953, 827-834.

[3] R.C Eberhart and Y. Shi, "Comparison between genetic algorithm and particle swarm optimization", in *Proc. IEEE int. Conf. Evol. Comput.*, 1998, 611-616.

[4] Zwe-Lee Gaing, "A Particle Swarm Optimization Approach for Optimum Design Of PID controller in AVR system", in *IEEE Transaction on energy conversion*, 19(2), 2004

[5] Dervis Karaboga and Bahriye Akay, "A comparative study of Artificial Bee Colony algorithm", in *Applied Mathematics and Computation*, 21(4), 2009,108-132

[6] Akhilesh Kumar Mishra, Navin Kuamr Singh, "Speed Control Of DC motor Using Artificial Bee Colony Optimization Technique", in *Universal Journal Of Electrical and Electronics* 1(3), 2013, 68-75.

[7] T.O Mahony, C.J Downing and K.Fatla,"Genetic Algorithm for PID

parameter Optimization: Minimizing Error Criteria", *process control and Instrumentation*, 2000, 148-153

[8] Jaspreet Kaur, Piyush Saxena and Dr. Prerna Gaur, "Genetic Algorithm Based Speed Control of Hybrid Vehicle" in *IEEE 978-1-4799-0192-0/13*, 2013

[9] X. S. Yang, "Firefly algorithm, stochastic test functions and design optimization," *International Journal of Bio-Inspired Computation*, 2(2), 2010, 78-84.

[10] D. Kumanan and B. Nagaraj, "Tuning of Proportional integral and derivative controller based on firefly algorithm" in *System Science & Control Engineering*, 1(1), 2013, 52-56.

[11] K.T. Oner, E. Cestinsoy, E. Sirimoglu, C. Hancer, T.Ayken, and M. Unel, "LQR and SMC stabilization of a new unmanned aerial vehicle" *world Academy of Science , Engineering and Technology* 58(1), 2009, 554-559.

[12] Gaddam MALLESHAM, Akula RAJANI, "Automatic Tuning Of PID Controller Using Fuzzy Logic" in *8th International Conference on Development And Application Systems Suceava, Romania*, 2006, 120-127.

Implementation and Comparative Analysis of Rotation Invariance Techniques in Fingerprint Recognition

Manisha Sharma^{*}, Deepa Verma^{**}

^{*}(Department Of Electronics and Communication Engineering, PTU, RBIET
Email: manisha21capricon@gmail.com)

^{**}(Department Of Electronics and Communication Engineering, PTU, RBIET
Email: deepaverma796@gmail.com)

ABSTRACT

In the image processing systems, the input image is first preprocessed, which may involve restoration, enhancement or just proper representation of the data. The most significant problem in image analysis is the detection of presence of an object within a given scene or an image. Such a problem occurs in trademarks classification and other areas like remote sensing for monitoring growth patterns within urban areas, weather prediction from satellite, target detection from radar or from the fighter plane etc. For this purpose template detection or template matching is the most commonly used technique. Using Rotation Invariant Template matching the object of interest can be easily searched even if it is rotated at any angle within the query image. In this paper, Rotation Invariant Template Matching is used for fingerprint identification, biomedical imaging, remote sensing and feature tracking.

Keywords: Biometrics, Fingerprint Recognition, Rotation

I. INTRODUCTION

Biometric system is an imperative area of research in recent years. Biometrics refers to the use of distinct physiological and behavioral characteristics to identify individuals automatically and has the ability to distinguish between an authorized person and imposter. Physiological characteristics include fingerprint, face, retina iris etc. and these characteristics are unique to every person [1]. Among all biometrics (e.g., face, fingerprint, hand geometry, iris, retina, signature, voice print, facial thermo gram, hand vein, gait, ear, odor, keystroke dynamics, etc.), fingerprint-based identification is one of the most mature and proven technique.

Nowadays, fingerprint recognition is one of the most important biometric technologies based on fingerprint distinctiveness, persistence and ease of acquisition. Although there are many real applications using this technology, its problems are still not fully solved, especially in poor quality fingerprint images and when low-cost acquisition devices with a small area are adopted. In fingerprint recognition process, the

important step which affects on system accuracy is matching between template and query fingerprint.

II. FINGERPRINT RECOGNITION

A fingerprint is comprised of ridges and valleys. The ridges are the dark area of the fingerprint and the valleys are the white area that exists between the ridges. Fingerprint recognition (sometimes referred to as dactylos copy) is the process of comparing questioned and known fingerprint against another fingerprint to determine if the impressions are from the same finger or palm. It includes two sub domains: one is fingerprint verification and the other is fingerprint identification. In addition, different from the manual approach for fingerprint recognition by experts, the fingerprint recognition here is referred as AFRS (Automatic Fingerprint Recognition System), which is program based.

However, in all fingerprint recognition problems, either verification (one to one matching) or identification (one to many matching), the underlining principles of well defined representation of a fingerprint and matching remains the same[2].

III. TRANSFORMS USED IN PROPOSED MODEL

Rotation invariant moments and transforms are such processes, which successfully deal with these situations. There are two types of rotation

transforms are sufficient to capture the essential features of an image.

The ORITs that were introduced in [3] include the polar complex exponential transforms (PCET), polar cosine transforms (PCT) and polar sine transforms (PST). These transforms are collectively known as PHTs. The difference between ORIMs and ORITs is that the radial parts of the kernel functions in ORIMs are polynomials and in ORITs these are sinusoidal functions.

The PHTs are preferred to ORIMs because PHTs are computationally very fast [4] and the high order transforms are numerically stable, whereas the ORIMs are less efficient and high order moments are numerically unstable. Because of their attractive features, PHTs have recently been used in many image processing applications. In [5], authors observed that PHTs-based features yield results comparable to state-of-the-art methods for fingerprint classification.

An extensive evaluation of invariance property of PHTs for image representation in terms of rotation, scale and noise has been conducted [6]. The authors observed that the ORITs are more suitable than ORIMs for applications, which require many features. The results are compared with ZMs and PZMs, and it is observed that the performance of PHTs is better than that of ZMs and PZMs.

The PHTs on Radon images for object recognition is applied [7] and the authors also compared their results with that obtained by ZMs, OFFMs and Radial Fourier Mellin moments. Through the theoretical analysis and experimental results, it is observed that the performance of PHTs for image description is much better than the three moments especially under noisy conditions.

invariant moments and transforms: orthogonal and non-orthogonal. The orthogonal rotation invariant moments (ORIMs) and orthogonal rotation invariant transforms (ORITs) are more effective in performance because they have minimum information redundancy and hence better information compactness. A few low order moments and

In this paper, we propose a method for the fast computation of the PHTs by developing recursive relations for the radial and angular parts of the kernel functions of the transform. An 8-way symmetry/anti-symmetry property is used to enhance the speed of the algorithm.

We have also studied the comparative analysis on these Rotational Invariant Techniques on basis of False Matching Ratio (FMR), False Rejection Ratio (FRR) or False Non-Matching Ratio (FNMR) and Accuracy.

IV. PERFORMANCE ANALYSIS

Fig 1 shows the steps implemented in the proposed model. Table 1 shows the False Acceptance Rate (FAR) and False Rejection Rate (FRR) at different Threshold values. The values in this table are obtained using first rotation Invariant technique known as Polar Sine Transform (PST) which varies at different angles (eg: 120, 145, 160). Table 2 shows the FAR and FRR at different Threshold values obtained using first rotation Invariant technique known as Polar Cosine Transform (PCT) which varies at different angles (eg: 120, 145, 160). Table 3 shows the FAR and FRR at different Threshold values obtained using first rotation Invariant technique known as Polar Cosine exponential Transform (PCET) which varies at different angles (eg: 120, 145, 160). Fig 2, Fig 3 and Fig 4 show the FAR & FRR with different values of Threshold on basis of PST, PCT, PCET respectively.

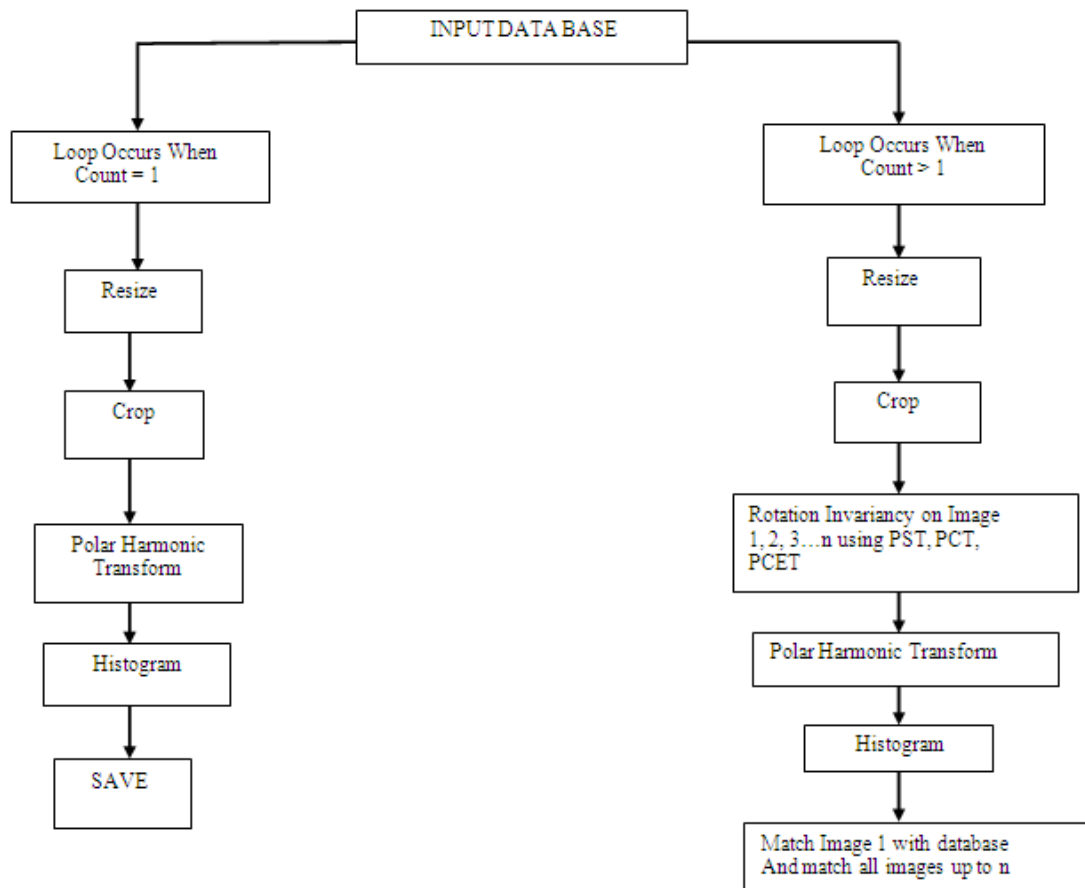


Figure 1: Framework of the Proposed Model

Table 1: PST Performance

	Threshold 1	Threshold 2	Threshold 3
Threshold	4	6	8
False Accept	0	3	6
False Accept %	50%	33.3%	25%
False Reject	0	3	6
False Reject %	50%	66.6%	75%
Accuracy	100%	50%	33%

Table 2: PCT Performance

	Threshold 1	Threshold 2	Threshold 3
Threshold	4	6	8
False Accept	3	3	0
False Accept %	0%	66.6%	75%
False Reject	3	3	0
False Reject %	100%	33.3%	25%
Accuracy	0%	100%	100%

Table 3: PCET Performance

	Threshold 1	Threshold 2	Threshold 3
Threshold	3	4	6
False Accept	0	2	0
False Accept %	33.3%	83.3%	66.6%
False Reject	0	2	0
False Reject %	66.6%	16.6%	33.3%
Accuracy	100%	125%	100%

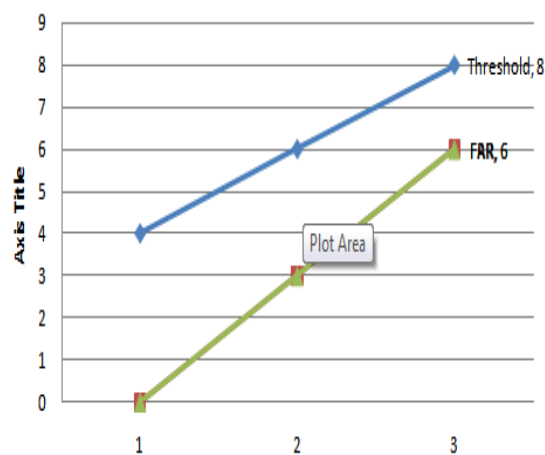


Figure 2: FAR & FRR vs. Threshold on basis of PST

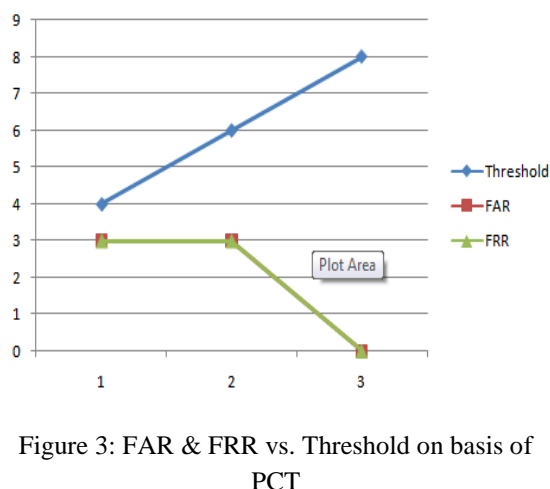


Figure 3: FAR & FRR vs. Threshold on basis of PCT

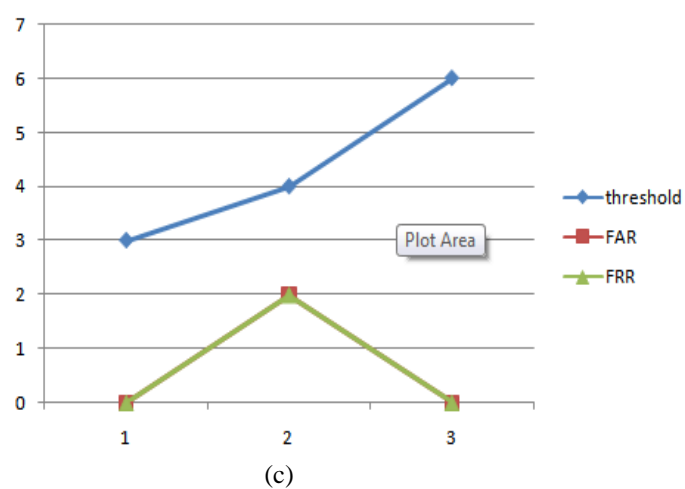


Figure 4: FAR & FRR vs. Threshold on basis of PCET

V. CONCLUSION AND FUTURE WORK

In this paper, we have presented rotation invariance in fingerprints by applying different techniques i.e. PHT, PCT, PCET. A fast method is developed in this paper for the calculation of PHTs. The comparison is made among all these three techniques with different threshold values and FAR, FRR are obtained by rotating images at different angles. This shows that the proposed method is suitable for applications where PHT coefficients are used as features in real-time environment involving large databases or on devices with low computation power. In future, these techniques can be used with Support Vector Machines (SVM) to provide better results.

REFERENCES

- [1] Dadgostar, M., Tabrizi, P. R., Fatemizadeh, E. and Soltanian Z. H, "Feature Extraction using Gabor Filter and Recursive Fisher Linear Discriminant with Application in Fingerprint Identification", *Seventh International Conference on Advances in Pattern Recognition, 2009*, 217- 220.
- [2] Sangram Bana and Davinder Kaur, "Fingerprint Recognition Using Image Segmentation", *International Journal of Advanced Engineering Sciences and Technologies*, 5(1), 2011, 012-023.
- [3] Yap, P.T., Jiang, X., Kot, A.C., "Two dimensional PHTs for invariant image representation", *IEEE Trans. Pattern Anal. Mach. Intell.*, 32(7), 2010, 1259–1270.
- [4] Yang, Z., Kamata, S., "Fast polar harmonic transforms", *Proceedings of 11th International Conference Control,*

Automation, Robotics and Vision, Singapore, 2010, 673–676.

- [5] Liu, M., Jiang, X., Kot, A.C., Yap, P.T., "Application of polar harmonic transforms to fingerprint classification", *Emerging Topics in Computer Vision and its Applications, World Scientific Publishing, Singapore, 2011*, 1-10.
- [6] Li, L., Li, S., Wang, G., Abraham, A., "An evaluation on circularly orthogonal moments for image representation", *Proceedings of International Conference of International Science and Technology, 2011*, 394– 397.
- [7] Miao, Q., Liu, J., Li, W., Shi, J., Wang, Y., "Three novel invariant moments based on radon and polar harmonic transform", *Opt. Commun.*, 285, 2012, 1044–1048.

Transmission Network Planning Using Evolutionary Programming

Rajanish kumar Kaushal*, Tilak Thakur**

*(Department of Electrical Engineering, PEC University of technology, Chandigarh (India)
Email: rajnish.nitham@gmail.com)

** (Department of Electrical Engineering, PEC University of technology, Chandigarh (India)
Email: tilakthakur20042005@yahoo.co.in)

ABSTRACT

This paper presents an application of Evolutionary Programming (EP) to solve Transmission Network Planning (TNP) in order to obtain the minimum cost solution while meeting the other constraints such as thermal, reliability criteria. The non-convexity that has been observed in the TNP cannot be solved effectively by conventional mathematical methods. EP has the ability to find the global optimal point in such a non-convex function. As there are no fractional transmission lines, TNP becomes a very complex mixed integer non-linear programming problem. EP can be used to select the optimal new transmission lines network with the least investment cost, while meeting the total load demands without any load curtailment.

Keywords – Evolutionary Programming, Minimum Cost, Transmission Network Planning

I. Introduction

India as a developing country, should improve the electricity supply all over the country. Because the amount of electricity supply is proportional to the economical, social development of a country. TNP is a very important topic considering India. If we can reduce the TNP cost while meeting the total load demands without any load curtailment and keeping maximum utilization of the total network capacity, will reduce the cost of electricity production. It is recognized that the allocation of transmission cost in a competitive environment requires careful evaluation of alternative transmission network plans. As a result, the need for methods that are able to synthesize optimal transmission network plans has become more important than ever. Unfortunately, practice has shown that conventional optimization procedures are unable to produce optimal solutions for networks. The reason is that the TNP problem is a hard, large-scale combinatorial problem. The number of options to be analyzed increases exponentially with the size of the network. The objective of TNP is to determine the installation plans of new facilities (mainly transmission lines) so that the resulting bulk power system may be able to meet the forecasted demand at the lowest cost, while satisfying prescribed technical, financial and reliability criteria. Although the conventional methods are somewhat successful in TNP, some problems still exist; Non-convexity: Due to non-convexity of TNP problem the

Success of the search largely depends on the starting point. Therefore, the optimization process sometimes stops at non-optimal solutions. Non-linearity: increases the iterations of the optimization algorithm and sometimes causes divergence [1].

A lot of research has been done using conventional mathematical methods to solve the TNP problem and some of the methods are:

Linear programming [2], Branch and bound [3], Benders and hierarchical decomposition [4], Heuristic and meta-heuristic methods [5], Simulated annealing [6], Hybrid Mathematical and Rule-based system [7], Tabu search [8], Genetic algorithms [9], Ant colony system algorithm [10].

II. INTRODUCTION TO TRANSMISSION EXPANSION PLANNING

The purpose of TNP is to determine the type of new transmission facilities required in order to provide adequate transmission network capacity to cope with the future generating capacity additions and load flow requirements. Main objectives of TNP are finding out the transmission network required to ensure reliable and stable power system while utilizing the maximum capacity of the network and estimating the minimum investment cost for the transmission network. This research work mainly focused on two transmission planning criteria named thermal criteria and minimum cost criteria.

$$P_p = \sum_{q=1}^n \{ep(epG_{pq} + fqB_{pq}) + fp(fpG_{pq} - epB_{pq})\} \quad (1)$$

$$Q_p = \sum_{q=1}^n \{fp(epG_{pq} + fqB_{pq}) - ep(fpG_{pq} - epB_{pq})\} \quad (2)$$

$$V_p^2 = e_p^2 + f_p^2 \quad (3)$$

Where P_p and Q_p are active power component and these three sets of equations (1), (2) and (3) are the load flow equations and it can be seen that they are non-linear equations in terms of the real and imaginary components of nodal voltages. Here the left hand quantities i.e. P_p , Q_p (for a load bus) and P_p and V_p for generator bus are specified and e_p and f_p are unknown quantities. For an n -bus system, the numbers of unknowns are $2(n-1)$ because the voltage at the slack bus is known and is kept fixed both in magnitude and phase. Therefore, if bus 1 is taken as the slack, the unknown variables are ($e_2, e_3, \dots, e_n, f_2, f_3, \dots, f_n$). Thus to solve the problem for $2(n-1)$ variables we need to solve $2(n-1)$ set of equations.

Since the TNP problem is nonlinear, iterative methods should be used to solve the problem. In this work the Newton-Raphson method has been used to solve the power flow problem. Newton-Raphson method is an iterative method which approximates the set of non-linear simultaneous equations to a set of linear simultaneous equations using Taylor's series expansion and the terms are limited to first approximation.

III. OVERVIEW OF EP'S THEORY

More than 45 years ago, several researchers from US and Europe independently came up with the idea of minimizing the mechanism of biological evolution in order to develop powerful algorithms for optimization and adaptation problems. This set of algorithms is known as evolutionary algorithms (EA). One of the most commonly used evolutionary algorithms is evolutionary programming (EP). The mathematical model of EP places emphasis on the biological linkage between parents and their offspring. EP obtains solutions to optimization problems using two basic operators: the mutation operator, which generates offspring by adding noise to the original structure of their corresponding parents; and the selection operator, which compares each member of the population (parent + offspring) with a number of randomly chosen opponents (from the population) to pick the individuals that will become parents for the next generation. This procedure is repeated for several generations, resulting in an evolutionary process that typically converges toward an optimal value.

The structure of the evolutionary programming [11] algorithm is shown in Fig 1. In this approach, the

real-valued decision variables to be determined are represented as a trail dimensioned vector. Each vector is an individual of the population to be evolved. The major steps involved in the evolutionary programming approach are explained as follows:

3.1 Initialization

An initial population of parent individuals ($PA_i, i = 1, 2, 3 \dots K$) is generated randomly within a feasible range in each dimension.

3.2 Creation of offspring (mutation)

Each parent vector PA_i generates an offspring vector by adding a Gaussian random variable with zero mean and pre-selected standard deviation to each individual of PA_i . The K parents create K offspring thus resulting in $2K$ individuals in the competing pool.

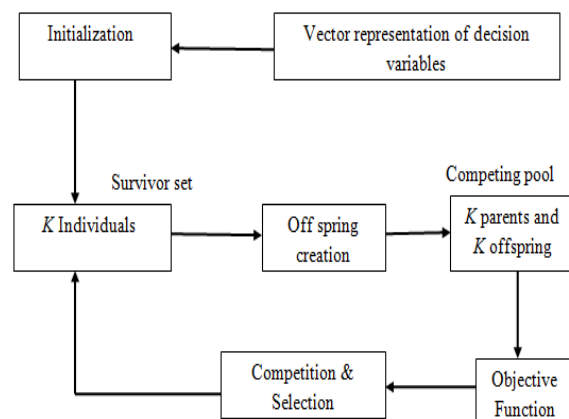


Fig 1: Structure of Evolutionary Programming

3.3 Competition and Selection

Each individual in the competing pool is evaluated for its fitness. All individuals compete with each other for selection. The best K individuals with maximum fitness values are retained to be parents of the next generation. The process of creating offspring and selecting those with maximum fitness are repeated until there is no appreciable improvement in the maximum fitness value or it is repeated up to a pre specified number of iterations.

IV. THE APPLICATION OF EP THEORIES TO SOLVE TNP PROBLEM (IMPLEMENTATION)

Fig 2 describes the steps of the implementation of the work "Transmission Network Planning using Evolutionary programming".

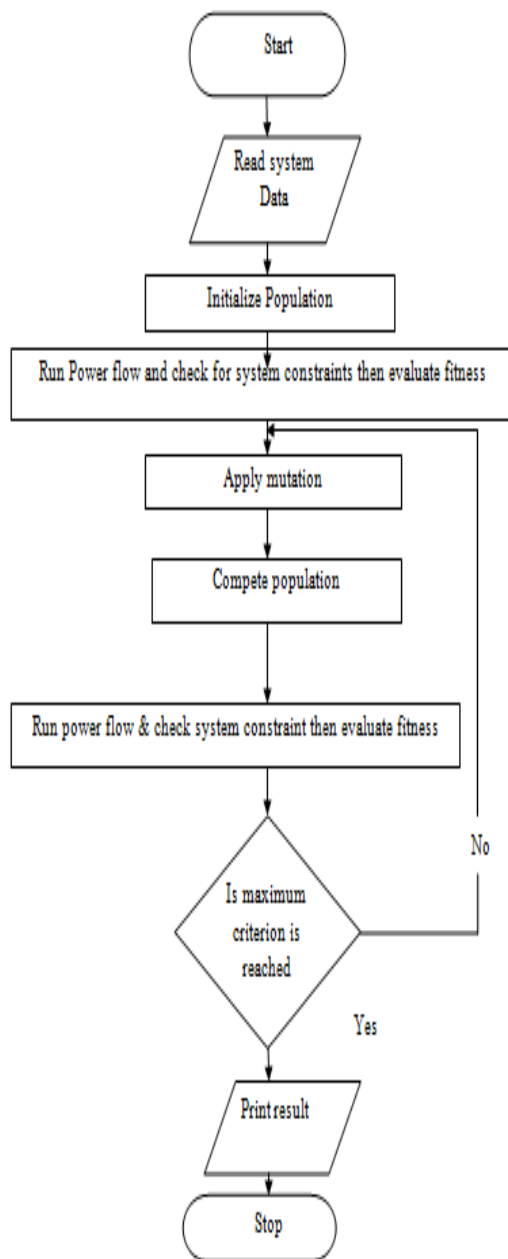


Fig 2: Flow chart of EP-TNP

4.1 Initialize the population

4.1.1 Representation

The value encoding method is used to represent the chromosomes. Each chromosome has 15 values to represent the all-possible transmission lines among six numbers of bus bars. The six bus bar network [1] as shown in Fig 3, has been used for this work.

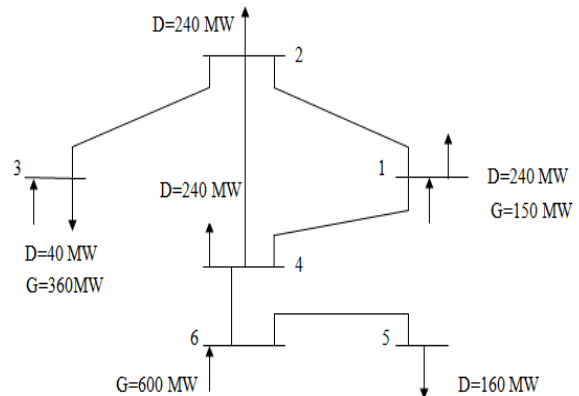


Fig 3: Six bus bar network

The program has used 10 different types of transmission cable types, i.e. 1xZebra, 2xZebra, 1xGoat, Lynx, Bear, 350 Oil Filled, 500 Oil Filled, 300 XLPE, 500 XLPE, 800 XLPE. To represent those line types 1 to 10 integers are used and to represent 0-line condition 0 integer is used in the program. The generations and loads of the six bus bar system are given in Table 1 and the properties of the line types are given in Table 2.

Table 1: Generation and Load

Bus	Generation capacity (MW)	Load(MW)
1	150	240
2	-	240
3	360	40
4	-	240
5	-	160
6	600	-

Table 2: The Properties of the Line Type

Line Type	Capacity (MVA)	Cost/km (Million Rs)	R Pu/km	X Pu/km
1xZebra	165	6	0.003	0.002
2xZebra	330	8	0.002	0.002
1xGoat	150	7	0.143	0.406
Lynx	105	5	0.001	0.002
Bear	130	7.5	0.075	0.190
350 Oil Filled	160	4.5	0.060	0.099
500 Oil Filled	120	4	0.051	0.095
300 XLPE	130	5	0.078	0.198
500 XLPE	160	4	0.048	0.182
800 XLPE	225	4.5	0.031	0.165

One of the possible chromosome \equiv
 100305600010060

1-2 Branch: 1xzebra, 1-5 Branch: 1xGoat, 2-3 Branch: Bear, 2-4 Branch: 350 Oil Filled, 3-5 Branch: 1xZebra, 4-6 Branch: Oil Filled and all other branches are not connected by a transmission lines.

4.2 Population Size

This parameter specifies the number of individuals in each generation of the EP. There are 20 chromosomes in a single population. So initial population is 2D matrix, the initial population is selected randomly. Size of the population doesn't change over time.

4.3 Load Flow Calculation

For the load flow calculation Newton Raphson method has been used. Main aim of performing the load flow calculation is to find the MVA flow in lines.

4.4 Fitness Evaluation

The objective of the thesis work is to use EP to obtain the optimized solution for TNP problem while achieving the minimum cost. So when mapping this objective to a fitness function, mainly three facts are considered; 1. To minimize the cost, 2.To reduce the number of over loaded lines, 3.To increase the line fitness of the network. The fitness function must reflect both the desired and the unwanted properties of a solution [12].

4.5 Minimize The Cost

Here consider the cost of transmission lines of the network. Transmission line types are varying basically according to its capacity & cost. So using EP, minimum cost transmission line can be selected, which suits to transfer required power between bus bars.

4.6 Reduce the Number of Over Loaded Lines

A transmission line whose power flow exceeds the capacity of it, called over loaded line. Over loaded transmission line is an adverse feature of a network. That means for the optimum network solution, we have to minimize or diminish the number of over loaded lines.

4.7 Line Fitness

Here line fitness means the number of lines in the network. The aim of inclusion of this parameter is to develop medium number of lines in the network while achieving the minimum cost.

4.8 Total Fitness of Population

For one generation the program runs for '20' number of chromosomes. Total fitness (TF) gives the cumulative sum of all 20 chromosomes fitnesses. Then there is a condition to check whether the total fitness of the new generation has improved or not when compared to the previous generation. If the total fitness of the new generation has improved, replace the previous generation with new population and its fitness values. If it has not improved, the previous generation and fitness values are backed up as new generation [13].

4.9 Mutation

The mutation operator, which generates offspring by adding noise to the original structure of their corresponding parents; and the selection operator, which compares each member of the population (parent + offspring) with a number of randomly chosen opponents (from the population) to pick the individuals that will become parents for the next generation. This procedure is repeated for several generations, resulting in an evolutionary process that typically converges toward an optimal value. EP seems to be promising and still evolving. Mutation process is used for creation of offspring from the parent chromosome [11]. In this process the number of offspring chromosome will be same as parent chromosome as shown in Fig 4. The main stages of the evolutionary programming based transmission network planning (EP-TNP) including initialization; mutation and competition.

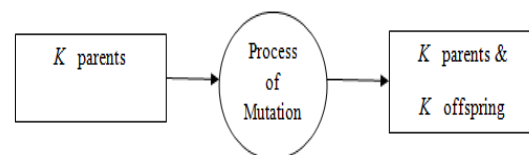


Fig 4: Creation of offsprings

V. RESULT

The combination which has the minimum cost that will be selected as the best combination of lines for the given generation and load is such as bus 1-2: 500 Oil Filled, bus 1-3: 1xGoat, bus 1-4: 800 XLPE, bus 1-5: 500 XLPE, bus 1-6: 800 XLPE, bus 2-3: 350 Oil Filled, bus 2-4: 300 XLPE, bus 2-5: 1xGoat, bus 2-6: Bear, bus 3-4: 300 XLPE, bus 3-5: 1xZebra, bus 3-6: 800 XLPE, bus 4-6: 300 XLPE, bus 5-6: 500 Oil Filled and the total cost for this combination is 4570 millions in rupees.

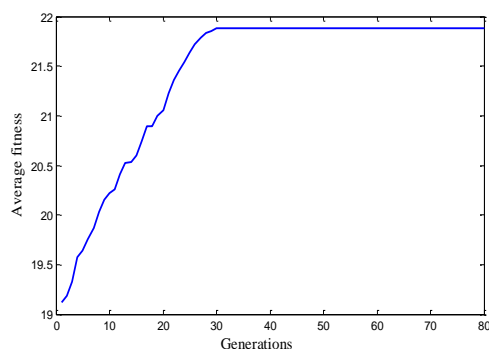


Fig 5: Average Fitness Vs Number of Generations

In Fig 5 the average fitness initially increases till approx 30 generations and it constant after approx 30 generations. It means that after, 30 generations there will be no improvement in the result, and the optimal combination of the lines for the given load and generation has been obtained.

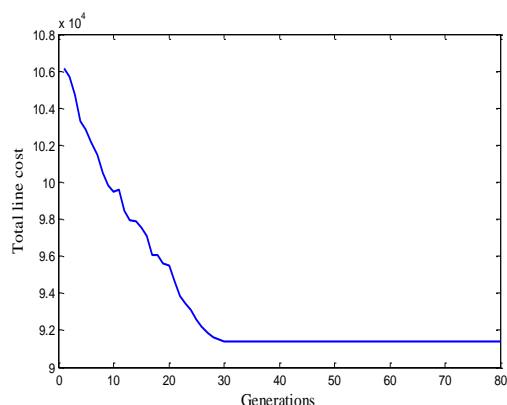


Fig 6: Total Line Cost Vs Number of Generations

Fig 6 represents the graph between total line cost and number of generations. In this the total line cost initially decreases till approx 30 generations and it constant after approx 30 generations. It means that the optimal combination of the lines for the given load and generation has been obtained. Here, total line cost is total sum of cost of parent chromosomes and fit offspring chromosomes.

VI. CONCLUSION

The research reported in this paper clearly demonstrates that an EP approach to a TNP problem is both feasible and advantageous. It provides to optimize several parameters in the same time. Furthermore, it allows the representation of non-linearities, which are hard to include in pure mathematical programming methods; in fact, the existence of non-linearities enhances the advantages of using EP against pure mathematical programming.

The results of an EP are a generation of solutions filtered through the struggle for survival. Therefore, many interesting and valuable exercises on comparisons and tradeoffs may be executed, helping the planner to gain insight on the problem he is faced with and allowing field for better decisions to be taken. Since EP problem starts with randomly generated solutions and all other operations randomly, we can obtained several different results for the same problem.

REFERENCES

- [1] M. T. A. P. Wickramarathna and N. Wickramaarachchi, "Transmission network planning using genetic algorithm", *IEEE/PES Transm. & Distrib. Conf. and Exposition*, 2006, 1-5.
- [2] L. L. Garver, "Transmission network estimation using linear programming", *IEEE Trans. Power App. Syst.*, 89 (7), 1970, 1688-1697.
- [3] S. Haffner, A. Monticelli, A. Garcia and R. Romero, "Specialised branch and bound algorithm for transmission network expansion planning", *IEEE Proc. Gener. Transm. & Distrib.*, 148(5), 2001, 482-488.
- [4] S. Binato, M. V. F. Pereira and S. Granville, "A new Benders decomposition approach to solve power transmission network design problems", *IEEE Trans. Power Syst.*, 16 (2), 2001, 235-240.
- [5] R. Romero, C. Rocha, J. R. S. Mantovani and I. G. Sanchez, "Constructive heuristic algorithm for the DC model in network transmission expansion planning", *IEEE Proc. Gener. Transm. & Distrib.*, 152 (2), 2005, 277-282.
- [6] R. Romero, R. A. Gallego and A. Monticelli, "Transmission system expansion planning by simulated annealing", *IEEE Trans. Power Syst.*, 11 (1), 1996, 364-369.
- [7] M. T. A. P. Wickramarathna, N. Wickramaarachchi, "Hybrid Mathematical and Rule-based System for Transmission network Planning in Open Access Schemes", *IEEE PES Transmission and Distribution Conference Exposition Latin America*, 2006, 1-5.
- [8] E. L. Silva, J. M. A. Ortiz, G. C. Oliveira and S. Binato, "Transmission network expansion planning under a tabu search approach", *IEEE Trans. Power Syst.*, 16 (1), 2001, 62-68.
- [9] D. E. Goldberg, "Genetic algorithm in search, optimization and machine learning", *Reading M. A. Addison Wesley*, 1989.

- [10] J. F. Gomez, H. M. Khodr, P. M. De Oliveira, L. Ocque, J. M. Yusta, R. Villasana and A. J. Urdaneta, "Ant colony system algorithm for the planning of primary distribution circuits", *IEEE Trans. Power Syst.*, 19 (2), 2004, 996-1004.
- [11] Y. R. Sood, "Evolutionary programming based optimal power flow and its validation for deregulated power system analysis", *Electrical Power and Energy Systems, Elsevier Science*, 29 (1), 2007, 65-75.
- [12] J. L. Ceciliano and R. Nieva, "Transmission network planning using evolutionary programming", *Proc. of The Congress on Evolution Computation (CEC 1999), Washington DC, U.S.A.*, 3 (1), 1999, 1796-1803.
- [13] Z. Michalewicz and M. Schoenauer, "Evolutionary algorithms for constrained parameter optimization problems", *Evolutionary Computation*, 4 (1), 1996, 1-32.
- [14] "Ceylon Electricity Board - Long Term Transmission Development Studies", *Technical Report, Asian Development Bank*, 2012.
- [15] "Matpower, a Matlab Power System Simulation Package", *User's Manual, Version 2.0*.